# Improved Characterization and Movement of the Platinum Band in a Proton Exchange Membrane Fuel Cell

by

David Luke Damron

B.Sc.E., Queen's University, 2013

A THESIS SUBMITTED IN PARTIAL FULFILLMENT OF

THE REQUIREMENTS FOR THE DEGREE OF

MASTER OF APPLIED SCIENCE

in

THE FACULTY OF GRADUATE AND POSTDOCTORAL STUDIES

(Mechanical Engineering)

THE UNIVERSITY OF BRITISH COLUMBIA

(Vancouver)

April 2016

## Abstract

Proton exchange membrane (PEM) fuel cells are devices that produce zero emission electricity, offering one pathway towards a sustainable energy future. They are in the early stages of commercialization in automotive, backup power and mobile power applications, with cost and lifetime of the cells still representing major barriers. Platinum (Pt) degradation in a PEM fuel cell leads to reduced performance and lifetime, while raw material costs represent a large portion of the overall cost. One of the Pt degradation modes leads to Pt dissolving from the cathode and precipitating in the membrane, forming a "Pt band". The Pt band is disconnected and unused Pt. If this Pt could be moved, it might be able to be returned to the cathode and be made useful again. This Pt can also have effects on membrane degradation.

Pt bands were created in two unique locations using accelerated stress tests (AST) of 10,000 square wave potential cycles from 0.6-1.0V. The locations of the bands were accurately predicted using an existing model and are dependent on the concentrations of oxygen and hydrogen in the membrane. It was hypothesized that increasing the oxygen concentration around the Pt particles in the membrane, would lead to dissolution and movement of the Pt. A new more quantified analysis of the Pt band using SEM imaging is implemented to measure the Pt movement and more fully characterize the Pt band. After two experiments, one trying to move the Pt for 28h and another for 100h, no Pt movement was observed. Another experiment created 2 Pt bands in the same membrane and characterized them for the first time. The second band formed in this experiment did not influence the first band, nor was it influenced by the first band during its formation. The new characterization techniques demonstrated that the distributions of

Pt mass and particles were different for the bands formed in the two different locations, while the dual band displayed a superposition of these distributions. The differences distributions have never been quantified before and could have different effects on membrane degradation, which should be the focus of future work.

## Preface

The work contained in this thesis, including all experiments, analysis and writing was conducted entirely by me, Luke Damron. Design of the experiments was developed with the help from Dr. Shankar Raman Dhanushkodi. All work was performed under the supervision of Dr. Walter Mérida.

A majority of the work contained in chapters 1-4 has been organized into a manuscript and submitted for peer review as a full scientific article titled: *Characterization of the Formation and Movement of the Platinum Band in a Proton Exchange Membrane Fuel Cell Using Image Analysis*. A portion preliminary results which became these chapters was presented at the EEST conference held at UBC in August 2015.

*Presentation reference:*

L. Damron, S. R. Dhanushkodi, W. Mérida. (2015) "Movement of the Pt band: an inside story." Presentation at the Electrochemical Energy Science and Technology conference, Vancouver, BC, August 18.

# Table of Contents

## List of Tables

## List of Figures

## List of Symbols

| | |
|---|---|
| $A_G$ | Geometric area |
| A | Atomic mass |
| Ω | Volume per atom |
| γ | Surface tension |
| D | Effective diffusivity |
| d | Particle diameter |
| $E^0$ | Standard-state reversible potential |
| $E_0$ | Accelerating voltage of electrons |
| $E_{GT}$ | Gibbs-Thomson energy |
| H | Henry's Law constants |
| K | Theoretical monolayer coverage of hydrogen |
| L | Platinum loading in catalyst layer |
| $p^0$ | Partial pressure |
| Q | Charge |
| ρ | Density |
| x | Dimensionless distance from cathode/membrane interface |
| Z | Atomic number |

## List of Abbreviations

| | |
|---|---|
| AST | Accelerated stress test |
| BOL | Beginning of life |
| BP | Backpressure |
| BPP | Bipolar Plate |
| BSE | Backscatter electrons |
| CCM | Catalyst coated membrane |
| CL | Catalyst layer |
| CV | Cyclic voltammetry |
| DAQ | Data acquisition |
| ECSA | Electrochemical surface area |
| EPTFE | Expanded tetrafluoroethylene |
| FCATS | Fuel cell automated test station |
| FRA | Frequency response analyzer |
| GDL | Gas diffusion layer |
| HOR | Hydrogen oxidation reaction |
| LSV | Linear sweep voltammetry |
| MEA | Membrane Electrode Assembly |
| MPL | Microporous layer |
| ORR | Oxygen reduction reaction |
| OCP | Open circuit potential |
| OCV | Open circuit voltage |
| PEM | Proton exchange membrane |
| PITM | Platinum in the membrane |
| Pt | Platinum |
| Pt/C | Platinum on carbon support |
| PTL | Porous transport layer |
| SE | Secondary electrons |
| SEM | Scanning electron microscope |
| TEM | Transmission electron microscope |

## Acknowledgements

I would like to thank my supervisor Dr. Walter Mérida for providing me with this amazing opportunity of pursuing my MASc at UBC. Thank you to UBC and NSERC for providing financial support throughout my studies.

Thanks Max and Devin for initiating me into UBC, helping me get set up in the lab, offering advice and sharing in intense (though often ridiculous) conversations. Thanks to Sebastian for struggling alongside me through the MASc process. I would also like to thank the other students in Dr. Mérida's lab who shared the frustrations of the Rusty Hut with me. Special thanks go to Dr. Shankar Dhanushkodi for giving me the initial ideas for the thesis and providing guidance along the way; I don't know where I would have been without you. Another special thanks to Dr. Gethin Owen for helping me with anything regarding the SEM, you were an invaluable resource.

I would also like to thank anyone else who helped either directly or indirectly throughout my time at UBC. Listening to my never ending ideas and rants cannot be easy; thank you Laura.

*For my mom,*

# Chapter 1: Introduction

Platinum (Pt) makes up a significant portion of the overall cost of proton exchange membrane (PEM) fuel cell systems. PEM fuel cells offer one pathway towards a sustainable energy future by creating electricity with zero emissions. Automotive fuel cells are in the early stages of commercialization and reduce $CO_2$ emissions in the transportation sector, a sector which currently makes up 14% of global emissions [1], and 23% in Canada [2]. Costs and lifetime of PEM fuel cells are currently barriers to commercialization for this technology; a deeper understanding of Pt degradation within the cell will help to design economically feasible, long-lasting fuel cells.

## 1.1 Basics: The Proton Exchange Membrane Fuel Cell

A proton exchange membrane fuel cell is one type of fuel cell, which uses hydrogen and oxygen to produce electricity, with water as the only by-product:

$$H_2 + \frac{1}{2}O_2 \qquad H_2O \tag{1.1}$$

The simplest PEM fuel cell uses two electrodes connected to an electric load, separated by a proton conducting membrane. Hydrogen and oxygen are fed to the electrodes and by only allowing hydrogen protons to pass through the membrane, the electrons are forced through the external circuit, powering the load. Figure 1 shows this basic layout of a PEM fuel cell:

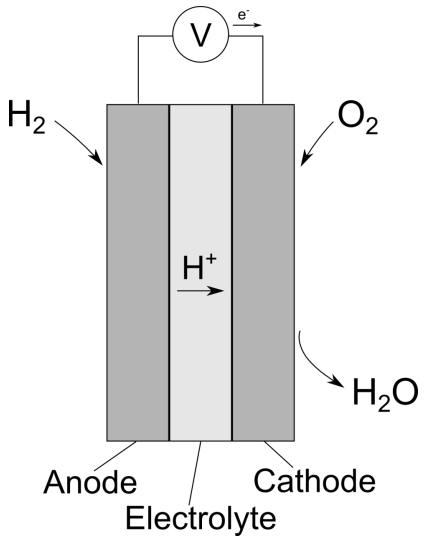


**Figure 1: Basic PEM fuel cell**

The electrochemical reactions happening at each electrode are half-cell reactions. In a PEM fuel cell the hydrogen oxidation reaction (HOR) occurs at the anode and oxygen reduction reaction (ORR) occurs at the cathode.

$$H_2 \rightarrow 2H^+ + 2e^- \quad (E^0 = \text{-}0.000\ V) \tag{1.2}$$

$$\frac{1}{2}O_2 + 2H^+ + 2e^- \rightarrow H_2O \quad (E^0 = 1.229\ V) \tag{1.3}$$

The potentials listed beside the half-cell reactions are the standard-state reversible potentials, where the hydrogen reduction reaction is often set to 0.0 V to be used as a reference to which other reactions can be compared. The standard potential of an electrochemical reaction is the sum of its half-cell reactions, 1.23 V in the case of a PEM fuel cell. This represents the ideal, reversible potential and is never achievable even in a perfect system due to the laws of

thermodynamics. In a real system, when current is drawn from the fuel cell to do electrical work lower, voltage losses reduce the cell voltage even more. The more current that is drawn, the more the voltage is reduced. A general relationship between the current and the voltage, called the polarization curve, is shown in Figure 2.

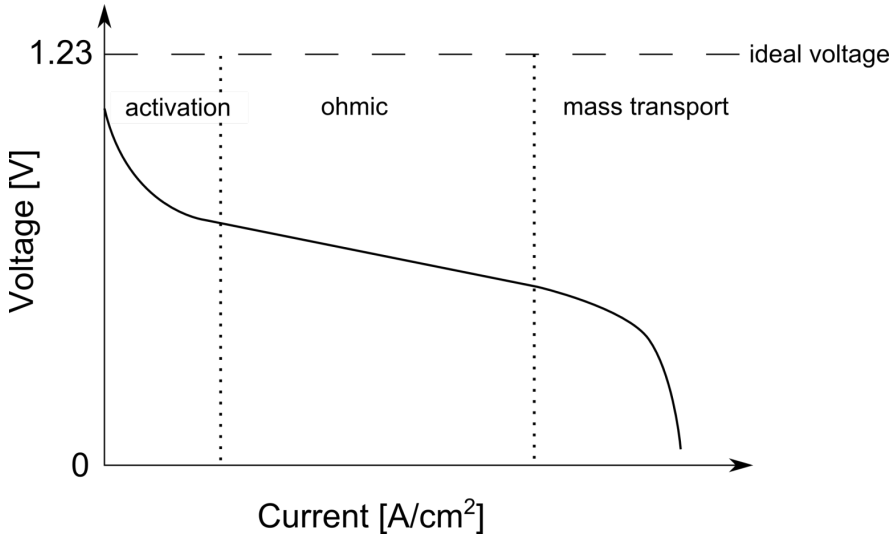


**Figure 2: General polarization curve of PEM fuel cell, showing activation, ohmic and mass transport regions**

The polarization curve has 3 main regions, which are described by the voltage loss mechanism that dominates the performance of the cell in this area of the curve. The regions are a) activation, b) ohmic and c) mass transport. It is important to note however that all of these losses are present at all operation points, but the effects are not always predominant. The focus of this thesis is on the activation loss region, which is related to the reaction kinetics and the catalyst. In order to produce cells with high voltage when current is drawn, fuel cells have been designed with specific materials that minimize these voltage loss mechanisms. Materials and their properties, as

well as their arrangement in the fuel cell are important for designing and developing cells with high performance. A general layout of a PEM fuel cell's components is shown in Figure 3.

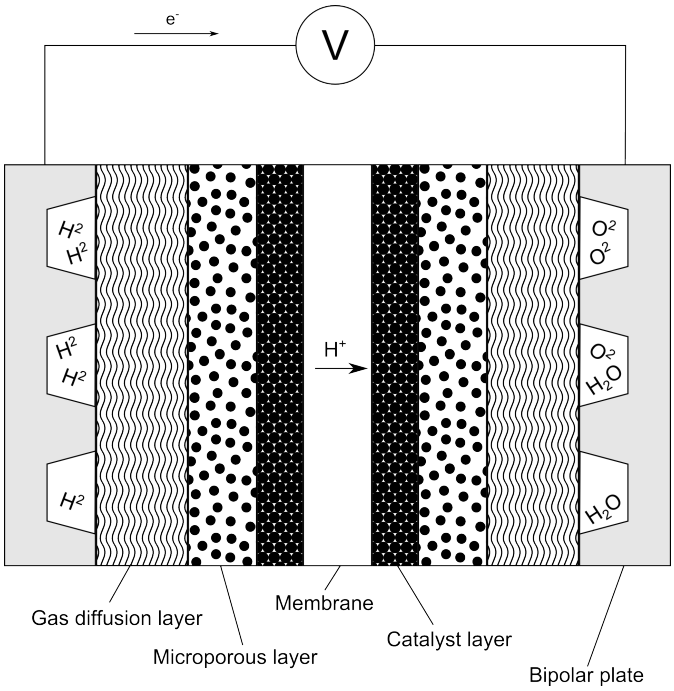


**Figure 3: Common PEM fuel cell layout**

As mentioned previously, the central component to the PEM cell is the membrane, which is a polymer (often Nafion™) is good at transporting protons but not electrons. A catalyst layers (CL) lies on both sides of the membrane which connect the membrane, electrode and void phases to facilitate easy movement of protons, electrons and reactants/products respectively; a catalyst is also introduced to increase the rate of the electrochemical reactions. Porous transport layers conduct electrons and allow gases and water to diffuse between the CL and the bipolar plates (BPP). They often consist of a highly porous carbon fibre layer, called a gas diffusion layer (GDL) with a less porous layer of carbon nanoparticles called a microporous layer applied to the

side in contact with the CL. The final layer is the BPP which is a conductive layer, such as graphite or stainless steel, with grooves through which the reactant gasses are fed. These layers make up a single cell. Cells can be stacked together to increase the voltage of the overall system, with the anode bipolar plate of one cell acting as the cathode plate of the adjacent cell -- hence bipolar plate.

The focus of this thesis is on Pt. The Pt is important for the activation losses shown in Figure 2, as the surface area is important for achieving a high performance cell. Furthermore, as the fuel cell operates the Pt can degrade, leading to permanent performance losses. Some of this Pt is transported into the membrane where it can affect the degradation of the membrane. Understanding the Pt in the membrane is the overarching concept of this thesis.

## 1.2 Background and Literature Review

The development of Pt as a catalyst in PEM fuel cells has been the subject of a lot of research over the years due to its high cost (~$900 USD per ounce as of Feb 2016). Until a cost effective replacement catalyst can be found (another area of intense research) which has sufficient performance and resistance to degradation, to compete with Pt, research in this area will continue to be a major focus within the PEM fuel cell research. This chapter will focus on more detailed Pt degradation background while also describing the current state of the research in this area, carving out a research gap into for this thesis to address.

### *1.2.1 Platinum in the Fuel Cell*

Catalysts are used in the fuel cell to increase the reaction rate by reducing the activation barrier of the reaction. A good catalyst will lead to better cell performance by reducing the losses in the activation loss region of the polarization curve, shown in Figure 2. Although many catalysts have been investigated for use in the PEM fuel cell, Pt/C (Pt on a carbon support structure) and Pt-alloyed catalysts remain the most common due to their low overpotential and high activity for the HOR and ORR reactions, while remaining resistant to the acid environment in the PEM fuel cell [3]. For effective use of the selected catalyst, it must be arranged methodically within the CL.

The CL consists of four phases: ionomer, catalyst, carbon and void space. Ionomer is more membrane like material that can transport $H^+$ to/from the membrane. The catalyst surface (the Pt) facilitates the electrochemical reaction, while transporting $e^-$ to/from the reaction. Carbon provides mechanical stability and creates a porous structure, while transporting $e^-$ to and from reactions. The void space is formed by pores in the CL structure and allows $H_2$ and $O_2$ gases, and $H_2O$ (liquid or gas) diffuse to and from the catalyst surface. The three CL materials must be organized to create reaction sites where all three phases are in contact, so all the reactants and products can be transported to and from the reaction through the appropriate phases. Where these phases meet are called triple phase boundaries. The composition of the CLs just described and the species transport within the cathode CL are shown in Figure 4 below. Maximizing triple phase boundaries is important to create an efficient cell; this is done by creating highly porous CLs with large catalyst surface areas. The CL is traditionally made using the decal method where ionomer, Pt/C and glycerol are mixed to form an ink on a Teflon backing, which is baked and

then hot pressed to the membrane before the Teflon backing is peeled away [4]. Newer techniques leverage inkjet printing to achieve more controllable CLs [5]. Maximizing the surface area of the Pt in the CL is important for high performance cells, but the amount of Pt must be minimized to keep down costs.

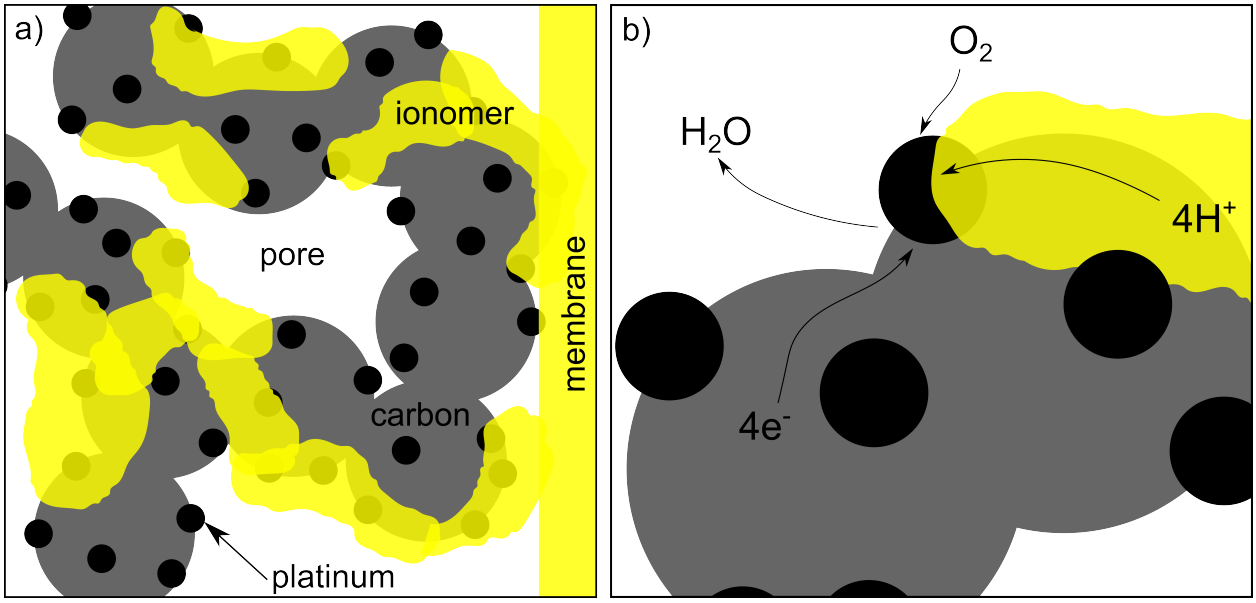


**Figure 4: Catalyst layer diagram. a) showing the components of the CL b) showing the transport of species in the cathode CL**

Depositing small Pt particles onto a carbon support (Pt/C) reduces the amount of Pt, while the carbon gives the CL structure and conducts electrons. By reducing the size of Pt particles, the surface area to volume ratio increases (due to scaling effects), reducing the mass of Pt needed to achieve the same surface area. The important metric is mg of Pt per $cm^2$ of the cell. Capability to create low Pt loading had already been increased by 100X from 4 $mg/cm^2$ in 1986 [6] to 0.04 $mg/cm^2$ in 2002 [7] and continues to improve by reducing particle diameters further. Unfortunately, reducing particle sizes decreases their stability due to increased surface energy.

Mean Pt particle size is often below 3 nm, and it has been found that the smaller the particles, the more degradation occurs [8]–[10]. Holby et al. suggest that increasing particle sizes slightly from common 2-3 nm range would have significant increases in stability [11]. Particle growth has been modeled with similar results [12]. This tradeoff between stability and performance vs Pt loading (cost) is critical for the commercialization of PEM fuel cells, which makes understanding the degradation of the Pt extremely important.

### *1.2.2 Platinum Degradation Mechanisms*

Long term operation of the fuel cell leads has been known for a long time to lead to a reduction in electrochemically active surface area (ECSA) of the Pt [13]. This reduces the area on which reactions can take place, reducing the cell performance. The mechanisms of Pt degradation have been developed more recently, most commonly described as a) detachment, b) coalescence/aggregation, c) electrochemical Ostwald ripening and d) dissolution and re-precipitation in the membrane. Detachment is Pt particles mechanically fall off the carbon support, usually due to carbon corrosion. Coalescence or aggregation occurs when Pt particles migrate and particles come in contact with one another, and remain stuck together. Electrochemical Ostwald ripening involves Pt dissolution, with precipitation back onto Pt particles; small particles are unstable and continue to dissolve more, while larger particles become more stable and continue to grow, leading to overall particle size growth. Dissolution with re-prepitation also involves first dissolution, but Pt ions are then transported into the membrane where they reduced by hydrogen diffusing through the membrane from the anode. Although all mechanisms lead to loss of ESCA, Ostwald ripening and Pt loss by dissolution have been found to be the most significant [14], [15]. Ferreira et al. estimate contributions are ~50%

for both Ostwald ripening and Pt dissolution with precipitation in the membrane [9], while others suggest the dominant mechanism between these two can be shifted base on the distance to the hydrogen sink [16], [17]. Reducing Pt dissolution is the most important to minimizing ECSA loss, as it is the first step in both of Ostwald ripening and precipitation in the membrane [18]. Pt that precipitates in the membrane is no longer active in the electrochemical reactions powering the fuel cell, and so is considered lost.

### *1.2.3 Platinum in the Membrane*

Dissolution of Pt can lead to particle growth via electrochemical Ostwald ripening, or be transported into the membrane where it precipitates. This Pt is often called PITM (Pt in the membrane). This occurs on the cathode CL, where the potential is high from the ORR (1.3). Pt in the membrane was first reported by Patterson [19]. A model has been developed by Darling and Meyers to describe the dissolution [20]; under high potentials, the Pt can undergo electrochemical or chemical dissolution via the following mechanisms:

$$Pt \rightarrow Pt^{2+} + 2e^{-} \tag{1.4}$$

$$Pt + H_2O \rightarrow PtO + 2H^{+} + 2e^{-} \tag{1.5}$$

$$PtO + 2H^{+} \rightarrow Pt^{2+} + H_2O \tag{1.6}$$

The $Pt^{2+}$ ions are then mobile, and can proceed to move into the membrane. There is some debate to the mechanism of transport; do the ions become complexed and are affected by migration [21]; are other species transported with the Pt [22]; does the Pt also diffuse as solid particles once

precipitated in the membrane [23]. Most however agree that it is the diffusion of $Pt^{2+}$ (though $Pt^{4+}$ can also be present [21]) and that these ions are reduced by $H_2$ diffusing through the membrane from the anode. The Pt ions can also deposit onto existing Pt particles, and are subsequently reduced by $H_2$. These steps are given by:

$$Pt^{2+} + H_2 \rightarrow Pt + 2H^+ \tag{1.7}$$

$$Pt_n + Pt^{2+} \rightarrow Pt_{n+1}^{2+} \tag{1.8}$$

$$Pt_{n+1}^{2+} + H_2 \rightarrow Pt_{n+1} + 2H^+ \tag{1.9}$$

With equation (1.7) describing the nucleation and equations (1.8) & (1.9) describing the growth of the particles. This growth mechanism is consistent with the finding single crystals in the membrane [9], [24].

The location of the Pt particle precipitation has been found to be affected by varying the amounts of $H_2$ and $O_2$ in the membrane [25]. Once the Pt is reduced/precipitated when it meets $H_2$ it becomes a surface on which reactions are catalyzed. These particles are not electrically connected, so they sit at open circuit potential (OCP). The reactions on the surface are the same HOR and ORR (equations that occur in the CL as the $H_2$ and $O_2$ diffuse through the membrane and reach the Pt particle surface. In the area near the cathode all of the $H_2$ is consumed, and the excess $O_2$ results in the particle having a very high OCP (~1V), such that it can cause the particle to undergo dissolution again. The Pt can move from the cathode CL in repeated dissolution then reduction cycles, diffusing while in ionic state [26], [27]. Eventually the Pt reaches a point where there is excess $H_2$, the HOR dominates and the potential drops near 0V. This is the location

where the Pt precipitates and remains. Pt particles continue to accumulate in this area, resulting in a formation a "Pt band". Zhang et al. and Bi et al. have developed models that predicts the band location based on the concentrations of $H_2$ and $O_2$ in the membrane, and have good agreement with experiments [28], [29]. The potential on the surface of the Pt particles along the thickness of the membrane has been estimated experimentally by using Pt wire probes [30], [31]. Models have been developed which show similar results [32], [33]. Although $O_2$ is said to dissolute the Pt, only Kim et al. have attempted to move the Pt using $O_2$ [27]; they claim to have caused some of the Pt in a previously made Pt band to move by increasing $O_2$ crossover, however they have no proper calibration of their experiment, nor any real quantification method. Platinum in the membrane, as a band or particles has been shown using TEM and/or SEM by many researchers, with only some of them listed here: [9], [10], [21], [24]–[26], [34]–[38]. Most of these researchers however only use the imaging techniques as a qualitative analysis, whether the Pt in the membrane is the focus of their work, or just confirmation of dissolution. Some of them measure the distance of the band, and thickness [27]–[29]. Only a few researches have applied more quantitative analysis to their imaging techniques in fuel cells [23], [39] or Pt precipitation in Nafion membranes [40]. Despite all of this research, the formation of the bands is still not that well understood, as some researchers have situations where no band is formed, or formed differently based on different membranes that are used [41]. In order to study the Pt band formation in a cost effective and timely manner, the degradation of the Pt must be accelerated in some fashion.

### *1.2.4 Accelerated Stress Tests*

Although long term operation of the fuel cell leads to decreased ECSA [13], this is impractical and costly for lab testing. Accelerating the degradation of the fuel cell by accelerated stress tests (ASTs) offers a way to perform lifetime testing in a significantly reduced time period, with specific methods needed to address Pt dissolution. Potential cycling has been found to cause dissolution into $Pt^{2+}$ when an oxidized Pt electrode is reduced in acidic media [42]. The mechanisms involved in Pt dissolution in acidic media are extremely complex [43], but in the fuel cell the Pt it has been generally found that increasing the potential of the cell leads to more dissolution on the cathode, up to about ~1.1V [44]. Higher temperatures during potential cycling have shown increased degradation rates of Pt [26]. Square wave potential profiles have been found to have the highest degradation rates for PEM fuel cells [45]. In another model by Darling and Meyers, they describe the oxidized platinum as protecting from dissolution under high potentials, but there is a potential window between $H_2$/air and air/air open circuit potentials where Pt is quite soluble [46]. Limiting the upper potential during cycling is important to limit carbon corrosion while focusing on Pt degradation [47].

### *1.2.5 A Note on Membrane Degradation*

The Pt that precipitates within the membrane is no longer active in the electrochemical reactions that power the cell, but as mentioned, the HOR and ORR are still catalyzed on the surface of these particles; these are not the only reactions however. Unwanted chemical reactions can be catalyzed on the surface, forming radicals which attack and degrade the membrane. This can cause the membrane to fail over time. These same radicals can also be catalyzed into other benign molecules, called quenching. The balance between these reactions is very important for

membrane life, and the relationship is relatively unknown. Some researchers show membrane degradation increases when Pt is impregnated in the membrane before operation [48], [49], while others show membrane degradation is mitigated [50]. Macauley et al. showed that with in-situ formed Pt bands (from fuel cell bus MEA) the membrane durability is enhanced [51], [52]. In a recent modeling abstract, Burlatsky & Atrazhev state low loading of small Pt particles causes fast membrane degradation, while high loading of large Pt particles act to mitigate membrane degradation [53]. Another work by Macauley et al. shows similar results experimentally [54]. Clearly the Pt has a complex relationship with membrane degradation and is not fully understood yet, though size and distribution very important.

### 1.3 Gap in Literature

Upon examination of the literature regarding Pt dissolution and precipitation in the membrane, it is evident that although there has been lots of work done, the complex phenomena involved are far from understood. Part of this is likely due to lack of quantified characterization of the Pt in them membrane; SEM and TEM are used effectively to measure some aspects of the Pt, but there is more that can be done with the image data that is can be collected with these techniques. Pt is supposedly transported with repeated oxidation/reduction from the cathode CL to the point where the Pt band develops. If that is true, there is a possibility for the particles to be made mobile again by increasing the oxygen concentration around the Pt. If the particles can be made mobile again it may be possible to move the Pt back to the CL where it can be made electrochemically active once more. One group has claimed to have moved the Pt [27], however they do not have a proper baseline to compare the “moved” Pt to, nor do they quantify the movement. Models have been developed which predict the location of the Pt band, but looking

closely at the band, it is clear that the band is a distribution of particles. This has not been quantified well either, and new research suggests that the size and distribution of particles is very important in relation to membrane degradation. There is a need for better characterization and understanding of the Pt distribution with the membrane so that cells can be operated in ways that do not increase the membrane degradation, or ideally, improve the membrane's resistance to degradation.

## 1.4 Objectives

The goal of this work is to improve the understanding of the Pt band in PEM fuel cells by addressing the research gaps in the area, identified in literature review. The work can be broken down into a few simple objectives, which are summarized as follows:

1. Develop ASTs which create Pt bands in multiple distinct and predictable locations
2. Move the Pt band precipitated in one location (by the AST) to another location using in-situ electrochemical techniques, without any further degradation to the cell
3. Apply new quantitative analysis to existing SEM imaging techniques, to provide a more quantitative description of the Pt band, and to measure any Pt movement

The following chapters will go on to describe the precise steps taken to address these objectives, including the experiments and techniques used. The results of these experiments are then discussed and conclusions are presented, along with recommendations for future work.

# Chapter 2: Experimental

This chapter explains the materials, equipment and experimental techniques that are used to study the Pt band. Electrochemical tests were performed in the fuel cell lab in the Clean Energy Research Centre, while SEM images were taken at the Centre for High Throughput Phenogenics and TEM images at the Bioimaging Facility. These facilities are all located at University of British Columbia's main Vancouver campus.

## 2.1 Materials

Each test used a new MEA, consisting of two materials: a gas diffusion layer (GDL) and a catalyst coated membrane (CCM). Commercial materials were used to better represent industrial fuel cells, while also having better reliability due to established manufacturing techniques. The porous transport layer (PTL) used was SGL 25 BC. It is manufactured by SGL group and consists of a GDL layer and a microporous layer (MPL). MPLs are commonly used as they have been found to increase performance. The material was chosen for its durability and its similarity to the material used in industry. Gore PRIMEA 5501 was used as the CCM. This material uses a Pt/C CL with symmetric 0.4 mg/cm$^2$ Pt loading on each electrode. It is a commercially available material and contains a layer of expanded tetrafluoroethylene (EPTFE) in the middle of the membrane, about 1/3 the overall thickness of the membrane.

## 2.2 Equipment

Experiments were conducted with a laboratory test cell, connected to a fuel cell test station. A potentiostat was connected to the cell to perform the electrochemical testing techniques.

### *2.2.1 Small Cell*

The experiments were performed using a laboratory test fuel cell with an active area of 2.25 $cm^2$. This is the 2D geometric area of that is available for each of the anode and cathode reactions. This cell was custom designed and manufactured in-house. It consisted most basically of graphite based bipolar plates, current collectors, a compression piston and thermocouples. Figure 5 shows the setup. Serpentine flow field channels are machined into the BPP delivering reactant gases on the sides in contact with the MEA while the opposite side had channels to circulate cooling/heating water. Holes drilled through the layers connected these channels with the bottom of the cell, where the inlet/outlet gases lines and inlet/outlet water lines. Seals keep the multiple gas and water pathways separate.

To assemble the fuel cell a brand new MEA is sandwiched between the anode and cathode bipolar plates so that the gases have access to each side of the MEA. Alignment was ensured using a custom built tool. All the layers were then compressed by supplying compressed nitrogen gas at 550 kPa to the compression piston.

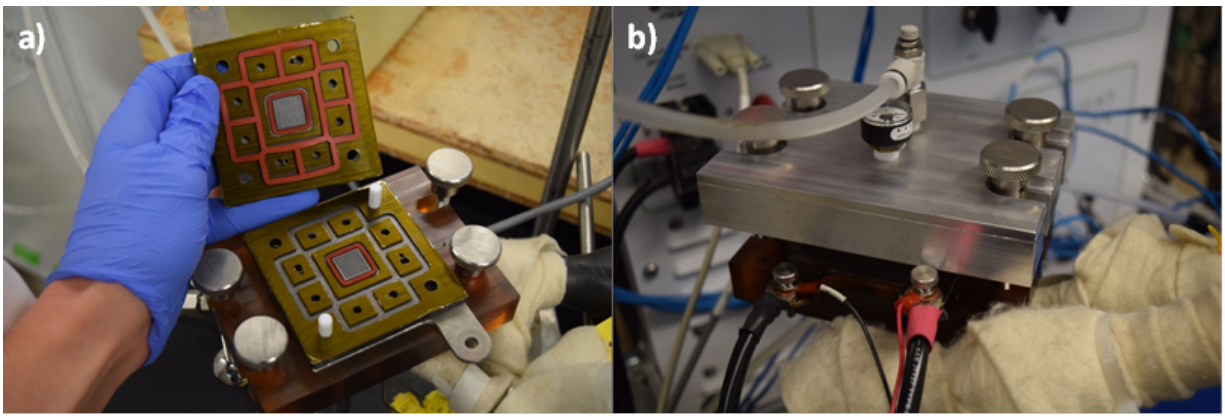


**Figure 5: Small cell hardware. a) Showing seals (orange), gas ports and active area (area inside square seal). b) Assembled cell with load cables**

### *2.2.2 Fuel Cell Test Station*

An FCATS-800W Greenlight fuel cell test station was used to provide the gasses for the fuel cell at the required temperature, pressure, humidity and flow rates. This machine is computer controlled with a DAQ and built in software accessible via the computer. All parameters can be set, monitored and recorded using the computer interface. The station was connected to the fuel cell with the proprietary hoses provided with the test station. Gases and electricity were supplied to the test station by the lab/building in which the station is operated. A load bank within the test station controls and monitors the voltage and current to and from the fuel cell, connected by electric cables from the station to the current collecting plates of the fuel cell. The station is shown in Figure 6.


**Figure 6: Greenlight FCATS-800W test station**

### *2.2.3 Solartron*

A Solartron 1470E potentiostat and FRA were used for superior control over potential cycling and the potential ramping needed for CV and LSV characterizations. This was due to the limitations of the load bank in the FCATS-800. The FCATS-800 station provided the gases while the load control was switched to this system by switching the load cables. These machines were connected together to a computer and using CorrWare software the parameters for the potential cycling and electrochemical characterizations (CV, LSV) can be set.

## 2.3 Electrochemical Techniques

Electrochemical techniques were performed using the FCATS-800 to provide gases at the desired flow rates, temperature, humidity and pressures while the Solartron potentiostat was used to set electrical loading conditions. Tests were all performed in-situ using the custom laboratory test cell. The conditions for the cell and the specifics for each experiment are outlined in table 1 and table 2, with the rest of this section explaining the details of this techniques and experiments.

**Table 1: Test station conditions for each electrochemical technique**

| *Technique* | *Cell Temp (°C)* | *Cathode BP (kPa)* | *Anode BP (kPa)* | *Hydrogen Flow Rate (nmlpm)* | *Air Flow rate (nmlpm)* | *RH (%)* |
|---|---|---|---|---|---|---|
| Conditioning | 60 | 100 | 100 | 200 | 500 | 100 |
| Polarization Curve | 60 | 100 | 100 | 200 | 500 | 100 |
| AST | 60 | Per Test | Per Test | 200 | 500 | 100 |
| CV | 60 | 100 | 100 | 203 | 623 (N2) | 100 |
| LSV | 60 | 100 | 100 | 203 | 623 (N2) | 100 |

**Table 2: AST experimental parameters**

| *Experiment* | *Description* | *Experiment Stage* | *Protocol* | *Cathode BP (kPa)* | *Anode BP (kPa)* |
|---|---|---|---|---|---|
| *1* | Baseline: Near | 1 | AST | 65 | 150 |
| *2* | Baseline: Far | 1 | AST | 150 | 50 |
| *3* | Reduced Oxygen Crossover | 1 | AST | 150 | 50 |
| | | 2 | 0.6V hold (28 h) | 65 | 150 |
| *4* | Pt band movement (28h) | 1 | AST | 65 | 150 |
| | | 2 | 0.6V hold (28 h) | 150 | 50 |
| *5* | Pt band movement (100h) | 1 | AST | 65 | 150 |
| | | 2 | 0.6V hold (100 h) | 150 | 50 |
| *6* | Dual Pt Bands | 1 | AST | 65 | 150 |
| | | 2 | AST | 150 | 50 |

### *2.3.1 AST*

Accelerated stress tests (ASTs) were used to induce Pt dissolution in a shorter operational time period. Tests consisted of 10,000 square wave potential cycles between 0.6-1.0V with 5s at each step. The square wave profile is used because it has been found to have the fastest rate of degradation [45], while 1V was used as the upper potential limit to mitigate the amount of carbon degradation. The test was stopped periodically to due performance tests and cell characterizations. The conditions for the cell during the ASTs are summarized in Table 1 and Table 2.

### *2.3.2 Polarization Curve*

The polarization curve measures the voltage response to a steady state current. The performance of the MEAs are measured using polarization curves periodically throughout the experiments after 0 cycles, 500 cycles, 1,000 cycles, 2,000 cycles and 10,000 cycles. These were controlled galvanostatically (i.e. controlling current), increasing the cell current from 0 A, stopping when the voltage dropped below 0.1 V. Voltage was measured every 0.05A from 0-1 A, then every 0.2 A after that. The conditions for the cell (flow rates, temperature, pressures, etc.) during the polarization curve are detailed in Table 1.

### *2.3.3 Cyclic Voltammetry*

Cyclic Voltammetry (CV) was used to measure the electrocatalytic surface area (ECSA) of the cell. This is the area of Pt available for use in the electrochemical reactions. The Solartron 1470E potentiostat was used to apply the voltage and measure the response signal. CVs were performed throughout the ASTs, measuring it at the same intervals as the polarization curves. ECSA was evaluated using cyclic voltammetry (CV) in $H_2/N_2$ mode. Cor-view software was then used to measure the hydrogen desorption peak's associated charge. This peak is shown in Figure 7. This charge is then input into the equation:

$$ECSA = \frac{Q}{K \times L \times A_G} \tag{1.10}$$

Where L is the loading for the Gore CCMs (L=0.4mg/cm$^2$) and the geometric area for the cell $A_g$=2.25 cm$^2$. K was taken to be 210 μC cm$^{-2}$ (theoretical monolayer coverage of hydrogen). The

cell conditions for this technique are given in Table 1, which followed conditions using in other work [55].

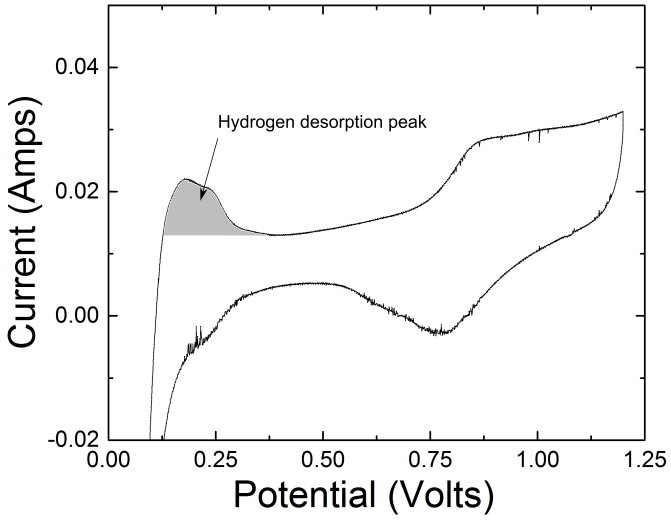


**Figure 7: CV profile for PEM fuel cell. Highlighted area is the hydrogen desorption peak, which is used for ECSA calculations**

### *2.3.4 LSV*

Linear sweep voltammetry (LSV) with $H_2$ at the anode and $N_2$ at the cathode was used to measure the $H_2$ crossover from anode to cathode as the platinum band developed, at the same intervals as CV and polarization curves. The same Solartron 1470E potentiostat was also used for the LSV. The crossover was determined from the current of the voltamogram at 0.35V. The cell conditions for the LSV are summarized in Table 1.

## 2.4 Morphological Techniques

Morphological techniques can be used to measure the location, size and shape of the Pt that has moved from the cathode CL into the membrane. In this work the main morphological technique used was scanning electron microscopy; however, some transmission electron microscopy was used as well. ImageJ was used to process and analyze all images from these techniques.

### *2.4.1 Scanning Electron Microscope*

The main characterization of the Pt in the membrane was performed using an FEI Helios NanoLab 650 scanning electron microscope (SEM). SEMs use a focused electron beam which is rastered across the surface of a conductive sample. The electron signal that is emitted from the sample is monitored by different sensors and the signal is used to create a greyscale image of the surface/topology of the sample in accordance with the location of the beam. The most common method, secondary electron (SE) mode, detects electrons which are emitted from atoms excited from the electron beam. These electrons are low energy and can only escape from atoms within several nm of the surface of the material being imaged. Edges allow a shorter path for these electrons to escape, leading to high contrast on angled surfaces. This mode is good for information of the surface of the sample. Backscatter electron (BSE) mode is another mode which uses elastic electron interaction to image the sample. Incident electrons are bent by interactions with the nuclei of atoms, usually in many small deflections, until the high energy electron is emitted from the surface of the sample and measured by the electron detector. These electrons travel much deeper into the sample and the fraction of electrons emitted is proportional to atomic number of the atoms. This leads to contrast in the SEM image based on atomic number. BSE can be used to image the Pt in the membrane due to the differences in atomic

number of the Pt and the carbon, fluorine, oxygen, hydrogen and sulfur atoms that make up the membrane.

For imaging the Pt, MEAs were cut with a scalpel and mounted in a holder so that the electron beam was perpendicular to the cross-section of the MEA. BSE mode was used to show sharp contrast of the Pt in the membrane. To limit the effect of the electron beam on the membrane, a low accelerating voltage and beam current were used of 5kV and 0.2 nA respectively. A close working distance of 2 mm was used to have high resolution. Figure 8 shows an example of the difference between BSE mode and standard SE mode; surface features are very visible in the SE image, with high contrast of edges, while the BSE mode shows the CLs in sharp contrast due to the Pt in these layers.

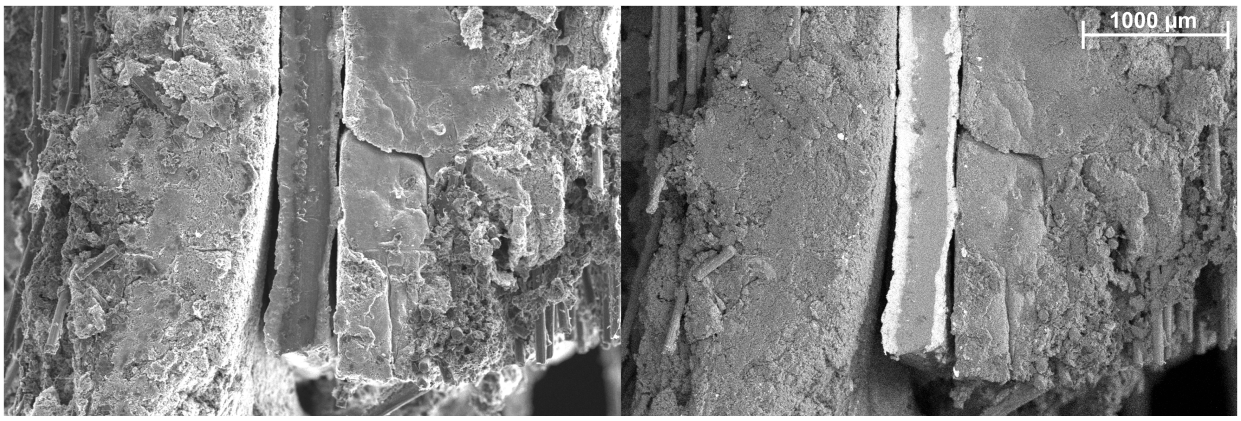


**Figure 8: SEM images. a) SE mode b) BSE mode showing the catalyst layers as white due to the Pt**

### *2.4.2 Transmission Electron Microscope*

Some samples were imaged using a transmission electron microscope (TEM). TEMs also use electron beams, but the beam must transmit through the sample, which means the samples have to be very thin. This sample preparation is tedious and time consuming, though the TEM does

offer greater resolution than the SEM. Higher resolution is achieved by the shorter wavelength of electrons when using higher accelerating voltages (ex: 200 kV vs 5 kV for TEM vs SEM). This is due to the de Broglie wavelength of electrons, which states electrons with higher momentum have a shorter wavelength.

For imaging MEAs, samples were set in epoxy to cure before being sliced into ~100nm thick samples using a microtome. A microtome uses a very small blade to slice a through the sample, and epoxy in which the sample is set, to create a thin sample for imaging. These prepared samples were placed on a copper grid which is inserted and imaged in an FEI Tecnai G2 TEM using 200 kV accelerating voltages.

### *2.4.3 ImageJ*

ImageJ is a free image processing software. It was used for processing and analyzing the SEM images of the particles. Using thresholding the greyscale images were converted to binary images before using a built in particle analysis tool to measure the area and position of the Pt particles. This data was then processed and analyzed further in MS Excel and Origin Pro.

## 2.5 Experimental Procedures

The steps for each experiment are very similar. First a new MEA is constructed and inserted into the fuel cell attached to the Greenlight FCATS. The test station is turned on ramping up all of the conditions in the cell such as temperature, flow rates, pressures and humidity. The cell is conditioned for 15 h at 0.6V before beginning any tests, any MEAs that don't achieve a performance of 1 $A/cm^2$ at 0.6V where thrown out. The BOL of the experiment is characterized

electrochemically using polarization curve, CV and LSV. The cell conditions are then changed and potential cycling begins. After a set number of cycles the AST is paused while another characterization step is performed. These two steps are alternated until the AST is complete. If there is a second stage to the experiments this begins and is followed by one last characterization step at the end of the second stage. All MEAs are then removed from the cell and taken to be imaged using the SEM. These steps are outlined in the flow chart in Figure 9. The fuel cell conditions for each test outlined in the flow chart are presented in Table 1 and Table 2.

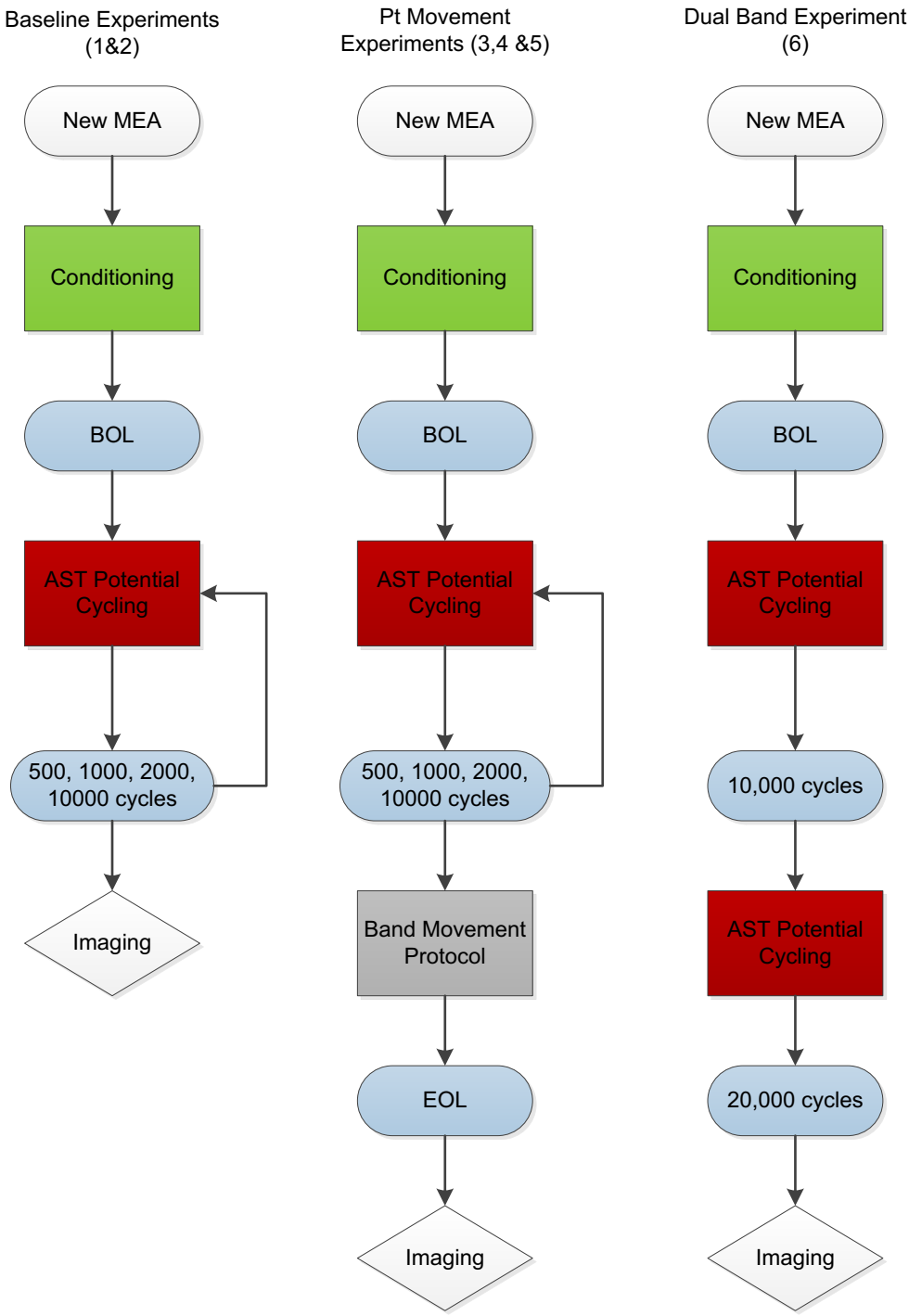


**Figure 9: Experimental procedure flow chart. Oval bubbles represent states, with blue bubbles being characterization steps. Square bubbles are test procedures (either AST or potential hold) and diamond bubbles are imaging using microscopy**

# Chapter 3: Results and Discussion

Experiments were developed to create Pt bands in PEM fuel cell membranes in-situ to approximate the Pt bands that form under extended use of cells under normal operating conditions. In-situ experiments to move these Pt bands are developed as well. The results of these experiments and discussions as they pertain to the objectives outlined in Chapter 1 are presented in this chapter.

## 3.1 Baseline Experiments

Before attempting to move the Pt in the membrane, baseline experiments were performed to first create Pt in membrane in distinct locations which could be measured and compared, while also monitoring the state of the cell with electrochemical techniques.

### *3.1.1 Applying Accelerated Stress Tests*

Accelerated stress tests were used to target the dissolution of platinum within reasonable timeframes. Square wave potential cycling was used as it has been found to have the highest degradation rate [45], with a potential profile of 0.6-1.0 V and dwell times of 5s. It was determined that 10,000 cycles was sufficient to cause significant Pt degradation with manageable experimental time. The state of the cell was monitored through CV and polarization curves throughout the experiments. Cell conditions such as anode and cathode flow rates, temperatures, BPs and humidity are outline in Table 1. All conditions are the same for every experiment, except for the BPs which are changed to affect $O_2$ and $H_2$ crossovers and the load control of the cell (for either AST or potential hold).

### *3.1.2 Platinum Surface Area Loss*

The Pt degradation of the cell was monitored during experiments by performing cyclic voltammetry at intervals of 0 (BOL), 500, 1000, 2000 and 10000 cycles. The CV curves during a 10,000 cycles AST is shown in Figure 10.

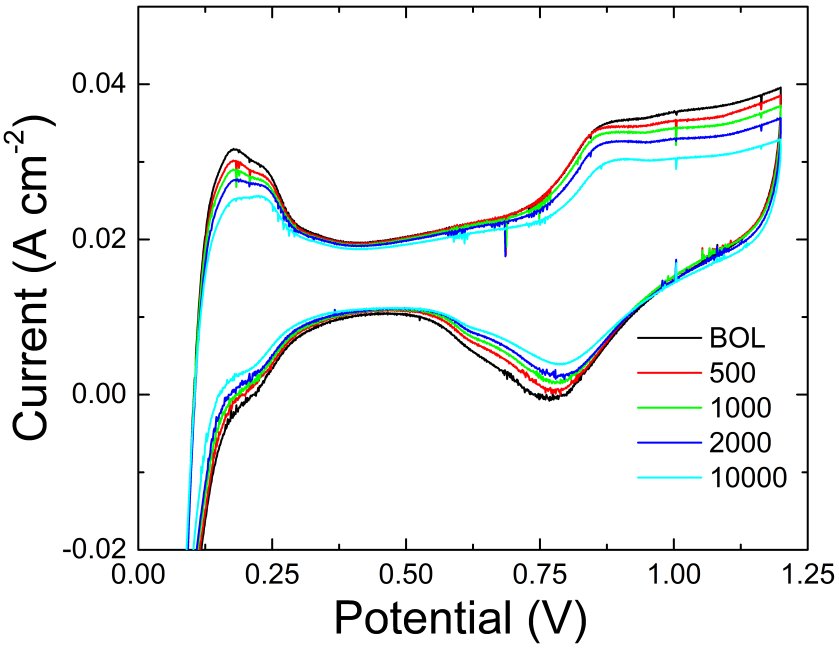


**Figure 10: CV curves performed at BOL, 500, 1000, 2000 and 10000 cycles showing a decrease in hydrogen desorption peak**

The ECSA of the Pt is calculated by integrating the area under the hydrogen desorption peak of the CV curve (top left of the CV curve) and using equation (1.10). The ECSA from these curves is computed and plotted in Figure 11.

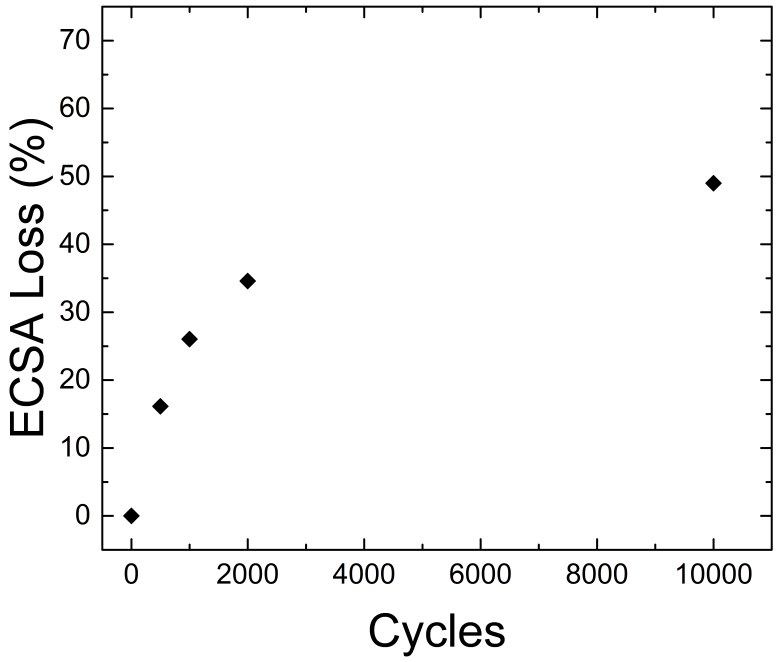


**Figure 11: ECSA loss on the cathode during AST plotted as percentage loss from BOL**

From Figure 11 it is clear that there is almost 50% loss of active area on the cathode, indicating a large amount of Pt degradation. Further analysis is needed to determine what happened to the surface area of the Pt in the cathode. It is expected that the majority of the losses are due to Pt growth (through Ostwald ripening) and dissolution with precipitation in the membrane [14], [15].

### *3.1.3 Platinum Particle Growth in the Catalyst Layer*

Electrochemical Ostwald ripening is responsible for ECSA loss in PEM fuel cells. Although this was not the focus of this work, TEM images were taken of the cathode CL to confirm this Pt degradation mode.

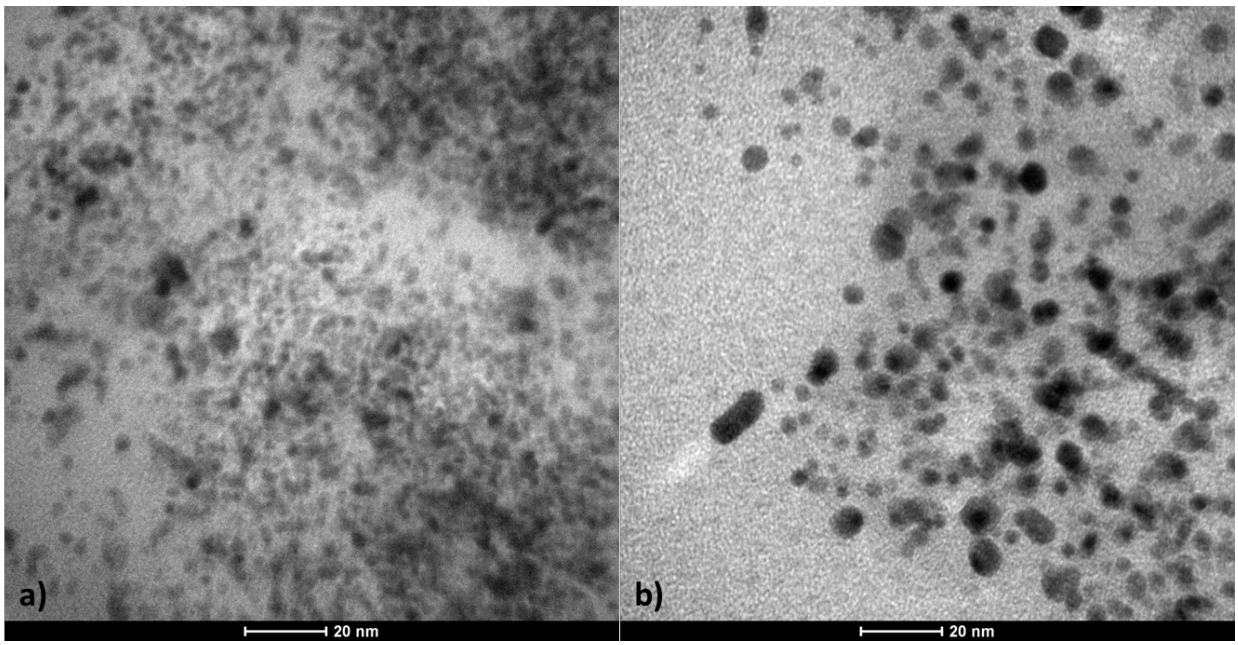


**Figure 12: TEM images of cathode CL. a) BOL b) 10,000 cycles (scale shows 20nm). Dark particles are the Pt particles**

Figure 12 shows the cathode CL at BOL and after 10,000 cycles; the black particles are the platinum nano-particles. It is clear that the Pt particles are much larger after 10,000 cycles, showing that the particles have grown over the duration of the AST. This accounts for some of the ECSA loss measured with the CV curves, while most of the rest is probably due to dissolution and migration of the Pt into the membrane. Others have estimated the growth and migration to account for about %50 each towards overall Pt surface area loss, with similar MEA and conditions [9]; the loss due to growth was not measured in this work.

### *3.1.4 Platinum in the Membrane*

Platinum degrades according to the 3-step dissolution model developed by Darling and Meyers [20]:

$$Pt \rightarrow Pt^{2+} + 2e^{-} \tag{1.11}$$

$$Pt + H_2O \rightarrow PtO + 2H^{+} + 2e^{-} \tag{1.12}$$

$$PtO + 2H^{+} \rightarrow Pt^{2+} + H_2O \tag{1.13}$$

The $Pt^{2+}$ ions are then mobile, and can proceed to move into the membrane where they are reduced by $H_2$ diffusing through the membrane from the anode. The Pt ions can also deposit onto existing Pt particles, and are subsequently reduced by $H_2$. These steps are given by:

$$Pt^{2+} + H_2 \rightarrow Pt + 2H^{+} \tag{1.14}$$

$$Pt_n + Pt^{2+} \rightarrow Pt_{n+1}^{2+} \tag{1.15}$$

$$Pt_{n+1}^{2+} + H_2 \rightarrow Pt_{n+1} + 2H^{+} \tag{1.16}$$

The $H_2$ is available due to the slight porosity of the membrane, which allows hydrogen to diffuse from the anode. The location of the Pt therefore depends on the $H_2$ permeating through the membrane. It has been found that the Pt particles accumulate in a uniform distance from the cathode, forming a band. This band location was discovered to be dependent on the $H_2$ as well as $O_2$ pressures in the electrodes [24], [28], [29]. Bi et al. and Zhang et al. developed models which predict the location of Pt precipitation [28], [29]. The model by Bi et al. is:

$$\frac{1}{x} = 1 + \frac{1}{2\alpha}\left(\frac{p_{H_2}^0}{p_{O_2}^0}\right) \tag{17}$$

Where x is the dimensionless distance from the cathode-membrane interface, $p_{O_2}^0$ and $p_{H_2}^0$ are the partial pressures of $O_2$ and $H_2$ at the membrane respectively and α is the is defined as:

$$\alpha = \frac{D_{O_2} H_{O_2}}{D_{H_2} H_{H_2}} \tag{18}$$

Where $D_{O_2}$ and $D_{H_2}$ are the effective diffusivities of $O_2$ and $H_2$ respectively, while $H_{O_2}$ and $H_{H_2}$ are Henry's Law constants. These models were used to estimate the location of the Pt band. The goal was to create two bands, each in their own distinct location before attempting to move the Pt bands in subsequent experiments. Figure 13 is a TEM image of the Pt particles formed in the membrane. This image shows a typical particle found in the membrane for this work. The sizes of these particles are ~90 nm in diameter and they have slight star shapes demonstrating signs of dendritic particle growth, which is commonly found in literature [25], [27].

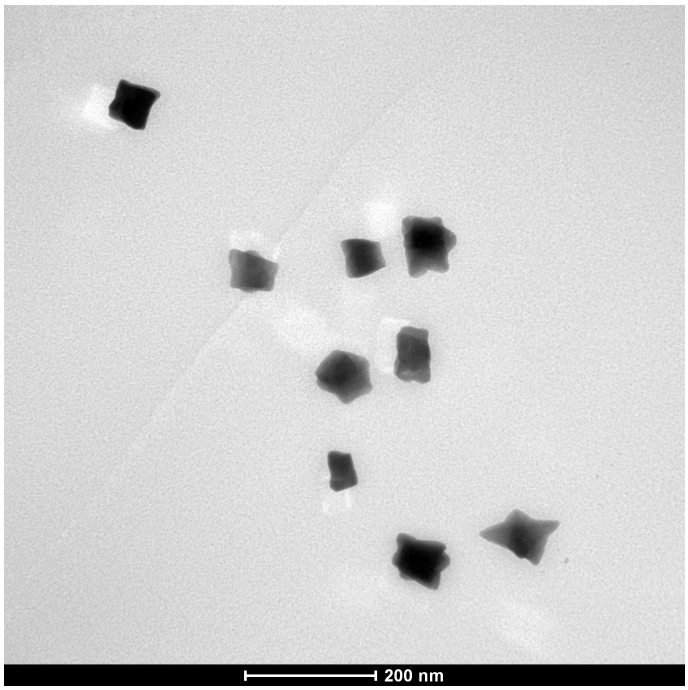


**Figure 13: TEM image of Pt particles in the membrane**

### *3.1.5 Platinum Bands*

Baseline platinum bands were created in distinct locations using the 10,000 cycle AST and different back pressures (BP) in the cathode and anode. A band was formed near the cathode using low cathode BP and high anode BP. A different band was formed further from the cathode

with a high cathode BP and low anode BP. The conditions for these two bands are described in Table 2.

After the ASTs are complete the Pt in the membrane is characterized by sectioning the MEA and imaging the cross-section in the SEM using BSE mode. In this mode, Pt appears in bright contrast against the carbon, hydrogen, fluorine, oxygen and sulfur which make up the sulfonated tetrafluoroethylene fuel cell membrane. The results for experiment 1 and 2 are shown in the following figures. The dotted line represents the predicted location using the model in equation (17) using the average membrane thickness which was measured to be ~20 µm.

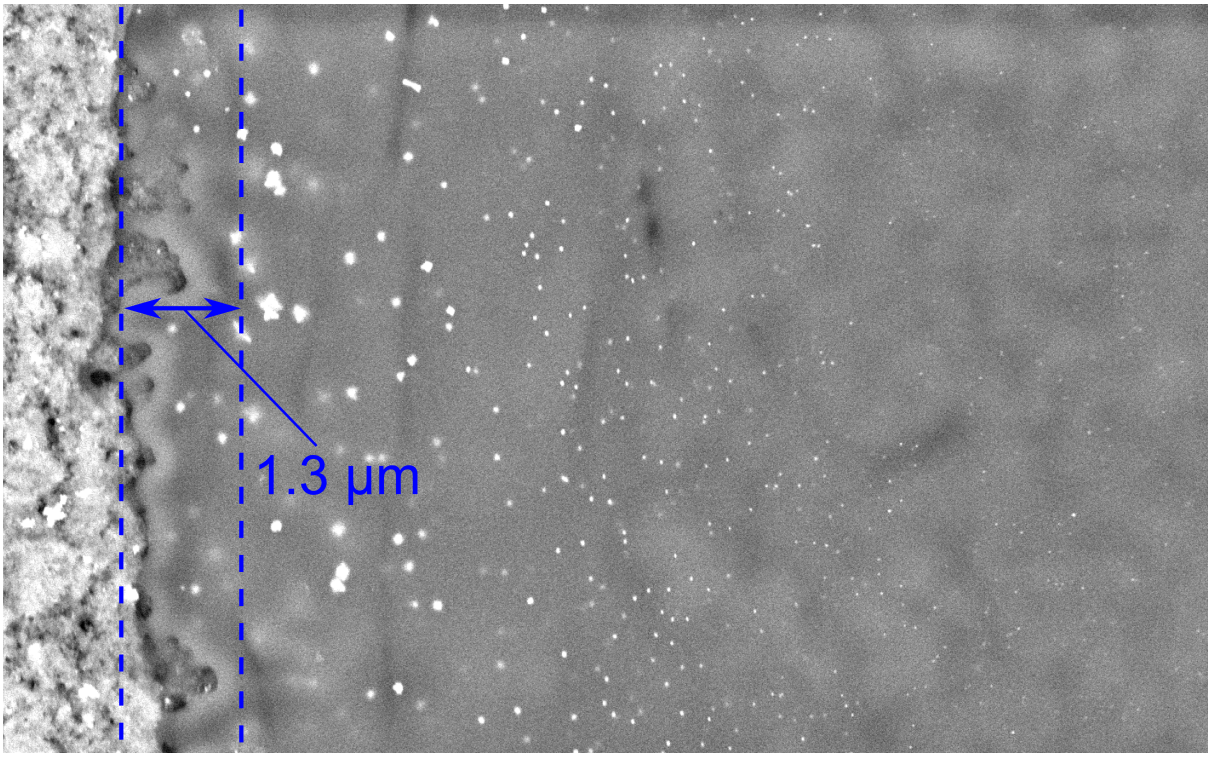


**Figure 14: SEM images of experiment 1, forming a Pt band near the cathode. Pt particles are white spots in the central membrane layer. Dotted line represents the predicted location of the Pt using the model**

Figure 14 and Figure 15 show partial agreement between the modeled and measured location if the location is taken to be the area containing the larges particles. It is very common for researchers to report Pt bands by measuring the distance of the Pt from one of the electrodes and sometimes describing the band with a thickness [27]–[29]. But looking at these two figures, it is clear that the Pt band is not really a band. The Pt "band" is an accumulation of particles, which can have a very wide distribution as shown here. It is known that the Pt band is widely distributed, and is especially obvious when using a TEM and with less developed bands (i.e. shorter test times).When using an SEM with lower magnifications and a very developed band containing a lot of Pt as many researchers do, the resulting image is often a bright band and they report it as such. They report a more macro characterization of the band, usually measuring the width and distance to the cathode. TEM is able to resolve the individual Pt particles of the band and characterize more micro characteristics of the band (i.e. particle size, shape, crystal structure) however the sample preparation is much more difficult and time consuming for using the TEM. TEM sample preparation also limits the number of locations along membrane which can be imaged because each sample is only spot only tens of micrometers wide (due to microtome procedure), while the SEM sample can be hundreds of micrometers long and can be imaged along the entire length. This allows many more SEM images to be taken of the same sample and average out the Pt band characteristics which can fluctuate along the MEA. The SEM available for this work (FEI Helios NanoLab 650 SEM) was able to resolve the individual Pt particles greater than ~9 nm in diameter (with a magnification small enough to capture all the particles in the band and the cathode's edge) with repeatable sample preparation and so was used in favor of a TEM. Using image analysis software, the individual particles were then analyzed to

get particle sizes and locations. After the methods for image analysis the smallest particle that could be resolved was 32 nm.

Although particles below 32 nm are counted at this magnification, due to the relationship between diameter and volume, the particles that are visible represent that majority of the mass of the Pt in the band, even if there are many more, smaller particles. The SEM images were compared to the few TEM images that were taken in this work and they did not show many Pt particles below this size.

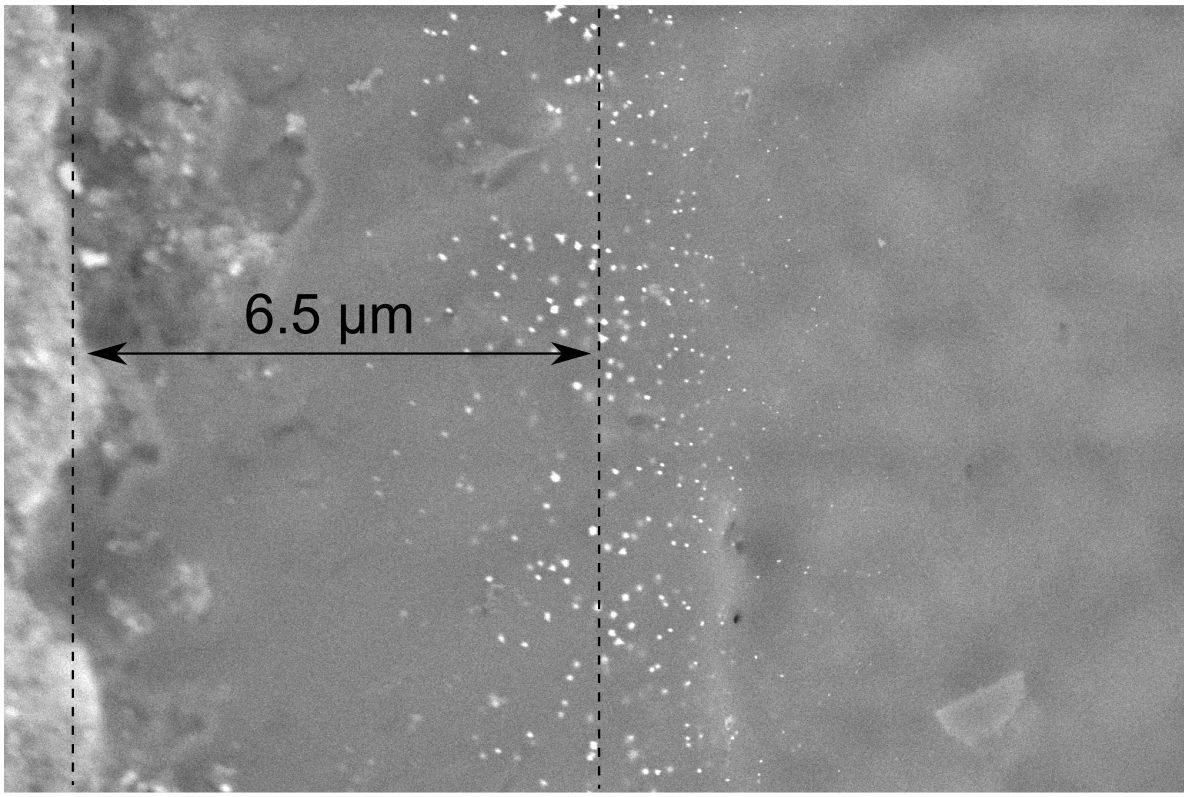


**Figure 15: SEM images of experiment 2, forming a Pt band near the cathode. Pt particles are white spots in the central membrane layer. Dotted line represents the predicted location of the Pt using the model (Pt is hard to see, but small amount behind dotted line)**

Processing the SEM images of the Pt bands was performed with ImageJ, and the size and location of each particle can was determined, giving much more information about the Pt "band". Figure 16 shows the process of converting a raw SEM image, with the binary image that is created in ImageJ and the particles that were counted using the built in particle analysis. The data output by the particle analysis was then processed and analyzed in other Excel and OriginLab. The same Pt bands shown in Figure 14 and Figure 15 can be represented with particle diameter and distance from the cathode CL. The results are shown in Figure 17 and Figure 18, making the band much easier to view and quantify.

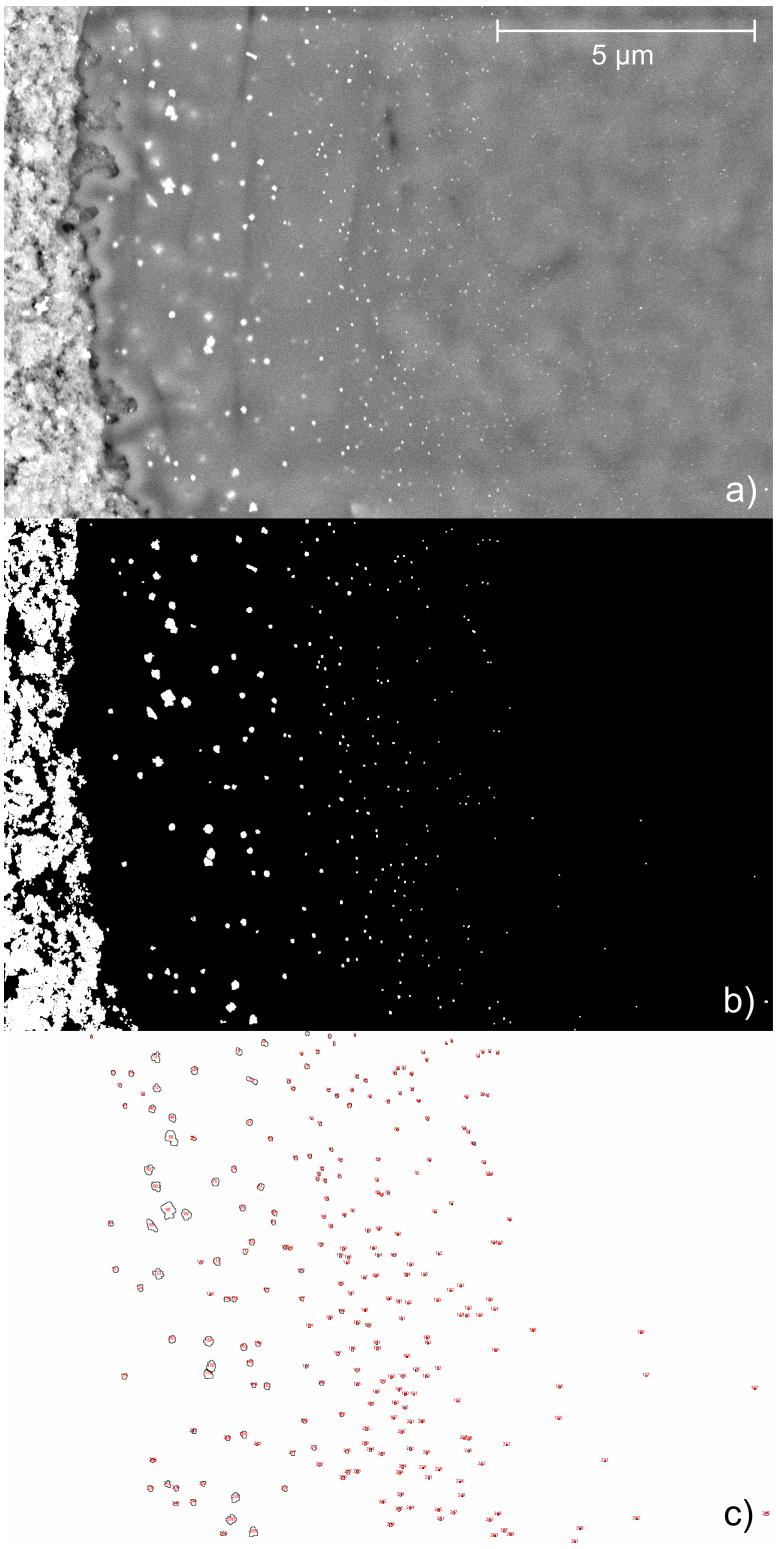


**Figure 16: Pt particle analysis using ImageJ. a) Raw SEM image b) Binary image intermediate created with ImageJ c) ImageJ particle analysis displaying the counted particles**

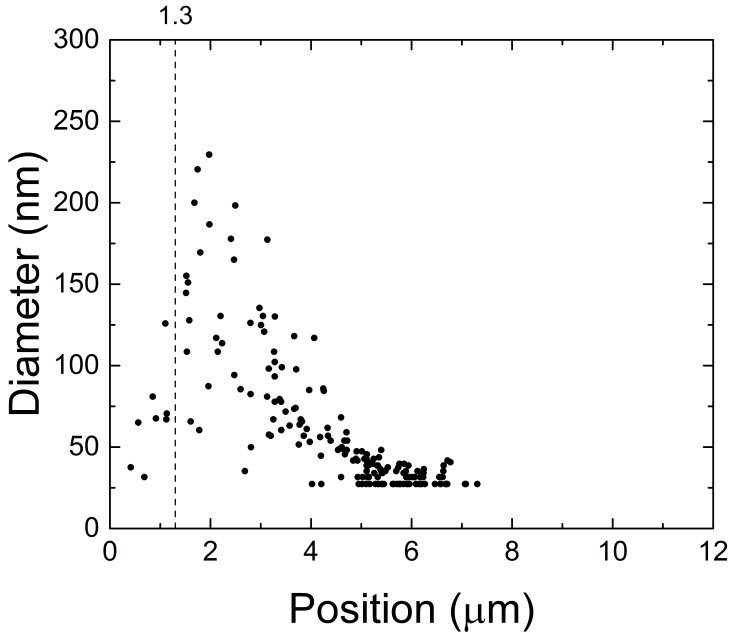


**Figure 17: Pt band from experiment 1 displayed as particle diameter vs location. Dashed line represents the predicted location using the model**

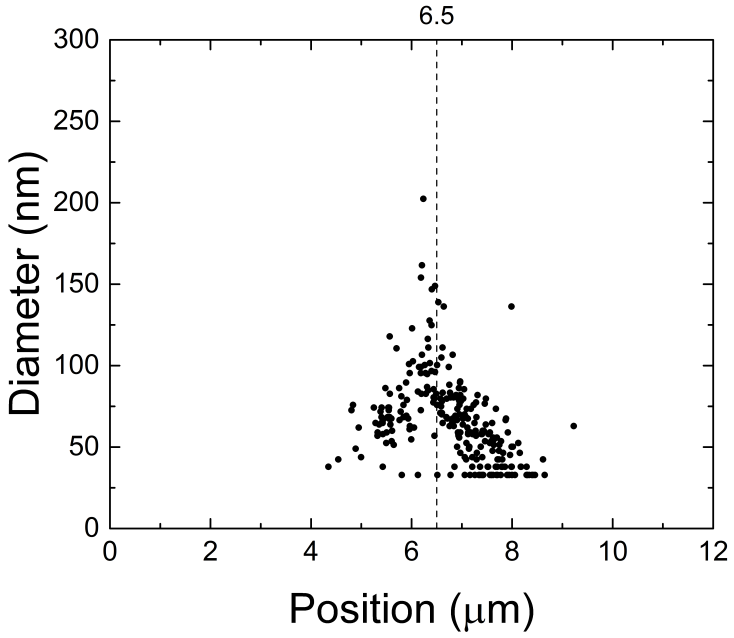


**Figure 18: Pt band from experiment 2 displayed as particles. Dashed line represents the predicted location using the model**

Figure 17 and Figure 18 show that the Pt bands are formed in two different distinct locations. The dotted line represents the predicted location of the band using equation (17). The model shows good agreement with the Pt bands if the location of the band is considered to be where the largest particles are formed. In the case of the band made far from the cathode shown in Figure 18, this represents the middle of the band with roughly equal distribution of particles on each side. In the case shown in Figure 17 the modeled location is near the largest particles, however the particles distribution is skewed away from the cathode and describing the band with using only distance to the cathode loses all the information about the particle distribution. Both Pt bands are more than "bands" and this will be discussed more later in the chapter. The data displayed in Figure 17 and Figure 18 will be used in the next stage of experiments to determine

whether the Pt band was moved and to better characterize the band than standard SEM imaging techniques.

The error and uncertainty of the Pt bands come from various sources. The experimental error involved, affects where the Pt forms in the membrane. This can be due to errors with the test station sensors (temperature, humidity, pressure), fluctuations of cell parameters (also temperature, humidity, pressure) and the differences of all of these parameters within the cell vs the test station where they are sensed and controlled. There is also error in the imaging of the samples, due to sample preparation, selecting the CL interface, instrument error of the SEM and resolution of the SEM. The MEA also is not perfectly manufactured (which affects the thickness and diffusion of the gases and Pt) and there is some randomness involved in all this. To reduce the most amount of error possible the most measurements possible were taken and averaging was used. The SEM allowed many images to be taken at different points along the membrane, and the most uniform sections of the membrane and Pt band were averaged.

### 3.2 Moving the Platinum Band

The Pt band model in equation (17) describes the location where the band will form, based on where $O_2$ and $H_2$ are in stoichiometric ratios. The reasoning for this is the potential of the Pt particles once they precipitate. Researchers suggest that Pt undergoes repeated oxidation and reduction as it moves from the CL to where the band precipitates [26], [27]. When the Pt is precipitates the new particle has a surface on which ORR and HOR reactions can catalyze. Near the cathode CL there is an abundance of $O_2$ and the ORR dominates the HOR on the particle (HOR is diffusion limited, ORR is kinetically limited). The particle is electrically disconnected so the potential approaches the OCV for the ORR reaction. This high potential causes the Pt to

undergo dissolution again, and the Pt ion continues to diffuse further from the cathode. Once the Pt is far enough from the cathode, the HOR begins to dominate (as the ORR is now diffusion limited) and the potential of the particle drops to near 0V. Platinum is very stable near 0V so the Pt remains a solid particle. The potential of Pt at different locations of the membrane have been measured [30], [31]. Mathematical models have been developed which show the theoretical potential of the Pt over the thickness of the membrane [32], [33]. The general shape of this Pt surface potential profile is shown in Figure 19.

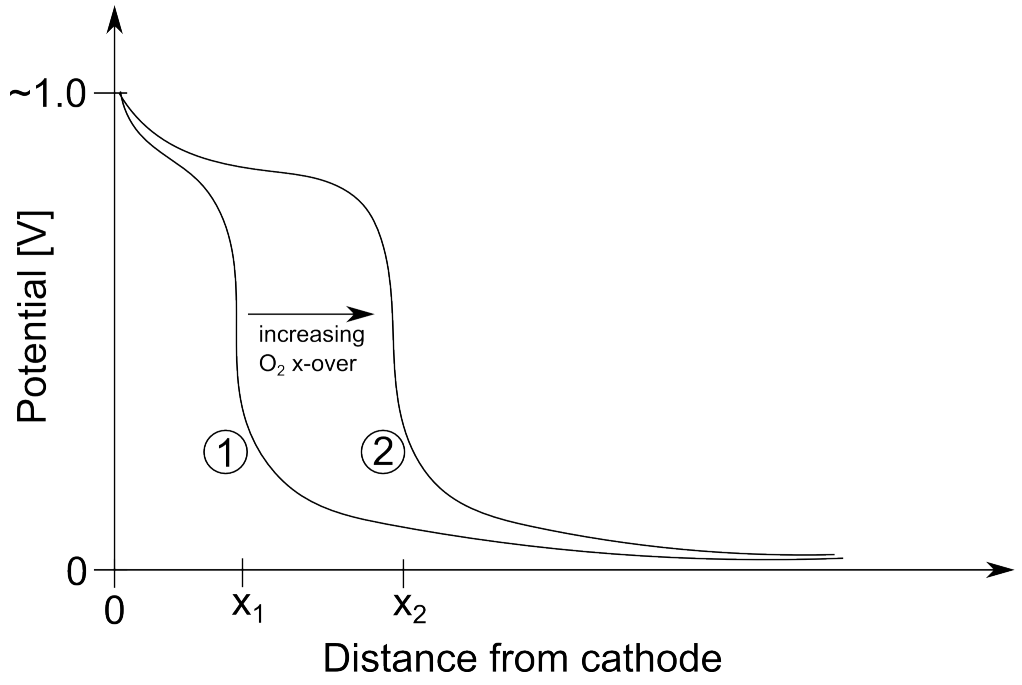


**Figure 19: Theoretical platinum surface potential profile as distance increases from cathode CL. 1 and 2 represent the near and far band locations formed in experiment 1 and 2 respectively**

The location of the large drop in potential is where $O_2$ and $H_2$ are in stoichiometric ratios and also where the Pt band forms. It was hypothesized that if a Pt band was formed at location 1 it could be moved to location 2 by increasing the $O_2$ crossover rate.

The Pt bands formed in experiment 1 and 2 were formed with a 10,000 cycle AST. To move these bands it should be possible to merely increase the $O_2$ crossover (by increasing the cathode BP) to put the particles in an $O_2$ rich environment and cause dissolution of the Pt particles already in the membrane. In order to determine that the Pt that is moved originates from the Pt band and not from the CL during the second stage of the experiment, the cell was operated at 0.6V (i.e. no AST) which is below the voltage which causes Pt dissolution. This lower voltage should also not affect the shape of the Pt surface potential profile as long as the permeation of $O_2$ and $H_2$ are not affected due to the cell using up more reactants, which would lower the concentration in the CL and reduce the diffusion rates across the membrane. To mitigate this, a very high stoichiometry was used, ~12 for both reactants at 0.6V. The test was run for 28h as this was roughly the time elapsed during the 10,000 cycles needed to form the band.

### *3.2.1 Decreased Oxygen Crossover*

The first experiment adjusting the $O_2$ crossover was not applied to move the Pt band, but to test that the cell would not degrade and that no additional Pt entered the membrane during the 28h of 0.6V potential hold. The first stage AST used conditions which formed the band in location 2, far from the cathode. The cell was then set to 0.6V and the BPs were changed to the conditions used in the AST of experiment 1. Any new Pt would then form in location 1 near the cathode due to the reduced $O_2$ crossover rate.

The ECSA of the sample remained relatively constant, increasing from 67.7% to 70.6% after the 0.6V hold stage of the experiment. The performance as measured by a polarization curve remained constant in the kinetic region of the curve and displayed only a very minor decrease in

the upper mass transport region. These results are shown in Figure 20 and Figure 21 respectively. These small losses are most likely just random error, but do not represent enough loss to influence future tests negatively. No new Pt was found forming in the membrane in location 1 near the cathode when the MEA was imaged in the SEM, which is where any new Pt would be expected. This helps confirm that the ECSA loss was just a measurement error, unless the loss was due to other mechanisms than dissolution; in either case a 0.6V hold will work as a non-destructive load control while the Pt movement protocol is applied.

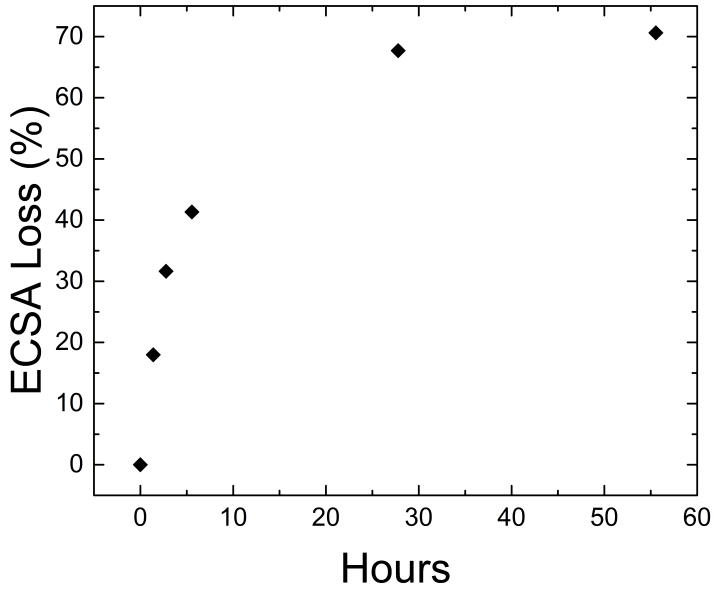


**Figure 20: ECSA during reduced oxygen crossover experiment. First 5 points are during AST, last point is after 28h of 0.6V potential hold**

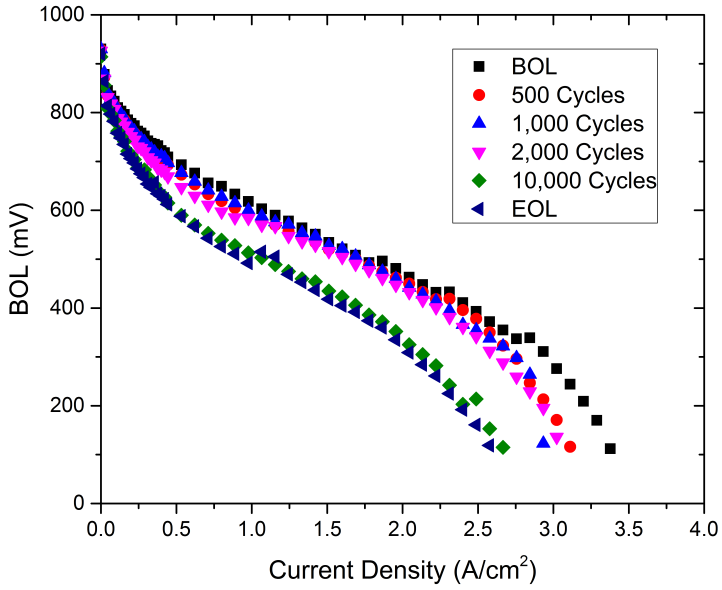


**Figure 21: Polarization curves during reduced oxygen crossover experiment. EOL is after 28h of 0.6V potential hold**

### *3.2.2 Increased Oxygen Crossover*

The increase of $O_2$ crossover while keeping the cell at 0.6V is considered the Pt movement protocol. The Pt band is first formed near the cathode about 1.3 µm away in location 1 with the same BPs as the first experiment (Cathode: 65 kPa, Anode: 150 kPa) using 10,000 potential cycles. The second stage of the experiment applies the Pt movement protocol to move the band. The BPs are changed to 150 kPa at the cathode and 50 at the anode, the same as in experiment 2. This increases the $O_2$ crossover and should shift the Pt surface potential profile shown in Figure 19 from location 1 to 2. The band formed in location 1 during the AST will be in an $O_2$ rich environment and prone to dissolution. The Pt becomes mobile when it is an ion, and diffuses

through the membrane where it should then precipitate in the new location of the large drop in the Pt surface potential profile, which is location 2 in this case, about 6.5 μm from the cathode.

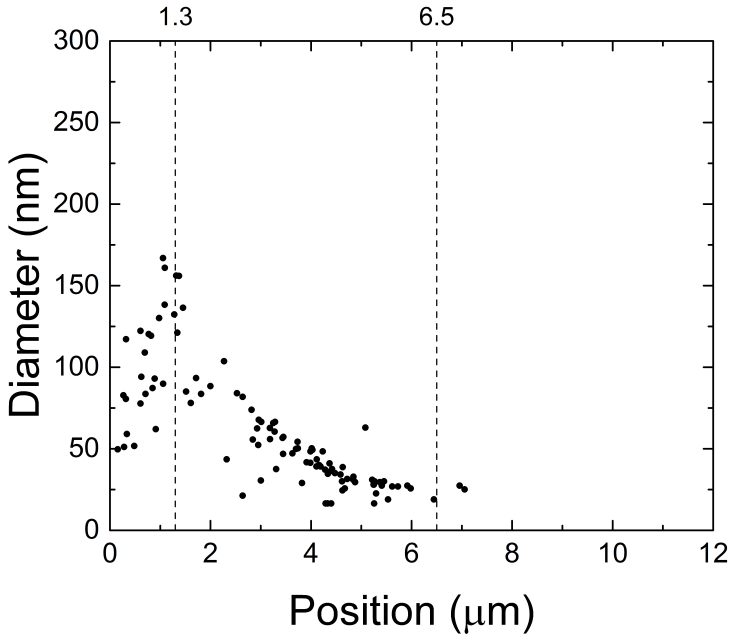


**Figure 22: Platinum movement experiment. 10,000 cycles followed by 28h Pt movement protocol. Dotted lines represent the predicted location of before and after movement**

Figure 22 shows the Pt particles after image processing. The band is formed where the model predicted during the AST portion of the experiment at 1.3 μm from the cathode. After the second stage of the experiment it is expected that any particles that underwent dissolution due to the increased $O_2$ crossover would precipitate around 6.5 μm from the cathode, as indicated on the figure. It does not appear that any Pt moved during this experiment. To investigate whether Pt dissolution might be occurring, just at a very slow rate, an extended Pt movement protocol was applied during the next experiment.

### *3.2.3 Extended Movement Protocol*

An extended Pt movement protocol was attempted to give more time the Pt to move, if perhaps the Pt movement was happening at a very slow rate which made it difficult to detect in the previous experiment. The extended Pt movement protocol was carried out the same as the first movement protocol, except the 0.6V hold stage of the experiment was extended from 28h to 100h. The results are plotted in Figure 23.

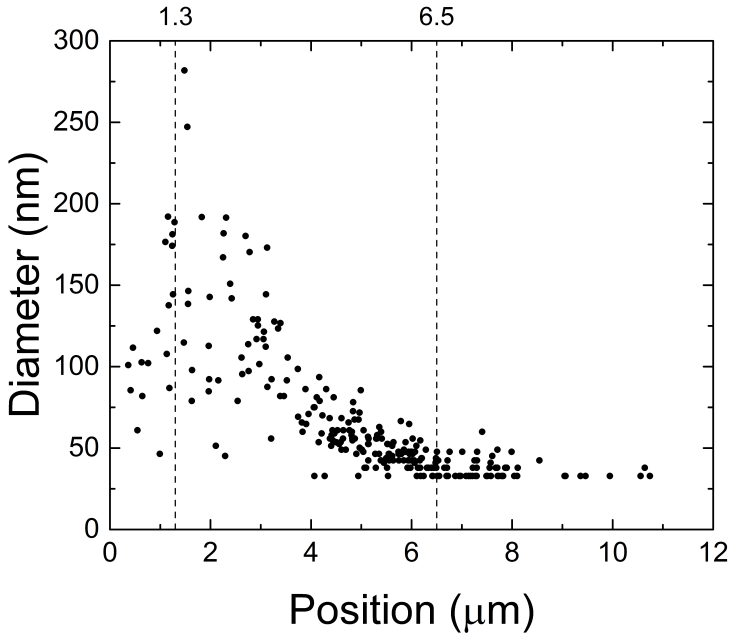


**Figure 23: Extended Pt movement experiment. 10,000 cycles followed by 100h Pt movement protocol. Dotted lines represent the predicted location of before and after movement**

The results after the extended Pt movement protocol do not appear much different to the first 28h movement protocol. In Figure 23 there are more Pt particles than Figure 22, however if the figure is compared with Figure 17, the number of particles is similar. This is partially due to the slightly lower quality SEM images used in creating Figure 22. Again there are large particles forming

around 1.3 μm from the cathode from the first stage AST, but there appears to be no large particles forming around 6.5 μm, which is location where $O_2$ and $H_2$ are in stoichiometric ratios during the movement protocol stage of the experiment. It would appear that under these conditions there is no Pt dissolution, or at least not perceptibly during a 100h time period, which is roughly 3.5X the time length needed to create the band initially. Overlaying the particle data from the three experiments to compare the bands is difficult due to the amount of data points. An easier comparison is made when the mass of Pt in the experiments is plotted by summing up the Pt particles for every 0.5 μm along the membrane thickness. The mass of Pt is also a more important parameter as it is the amount that has left the cathode, however the Pt surface area and number of particles is significant because it is where the reactions are catalyzed. The implications of the particles vs mass are discussed later in the chapter. In order to reduce error of measuring the distance of the particles to the cathode and the slight variations in the bands due to randomness, 3 images from each experiment were averaged for all mass data. Normalized mass is used to compare the masses as adjustments in focus shift the focal plane (when focusing SEM) can reveal more or less Pt particles if the focus is not identical; it is the relative position of the Pt, not the absolute mass that is of interest for this work.

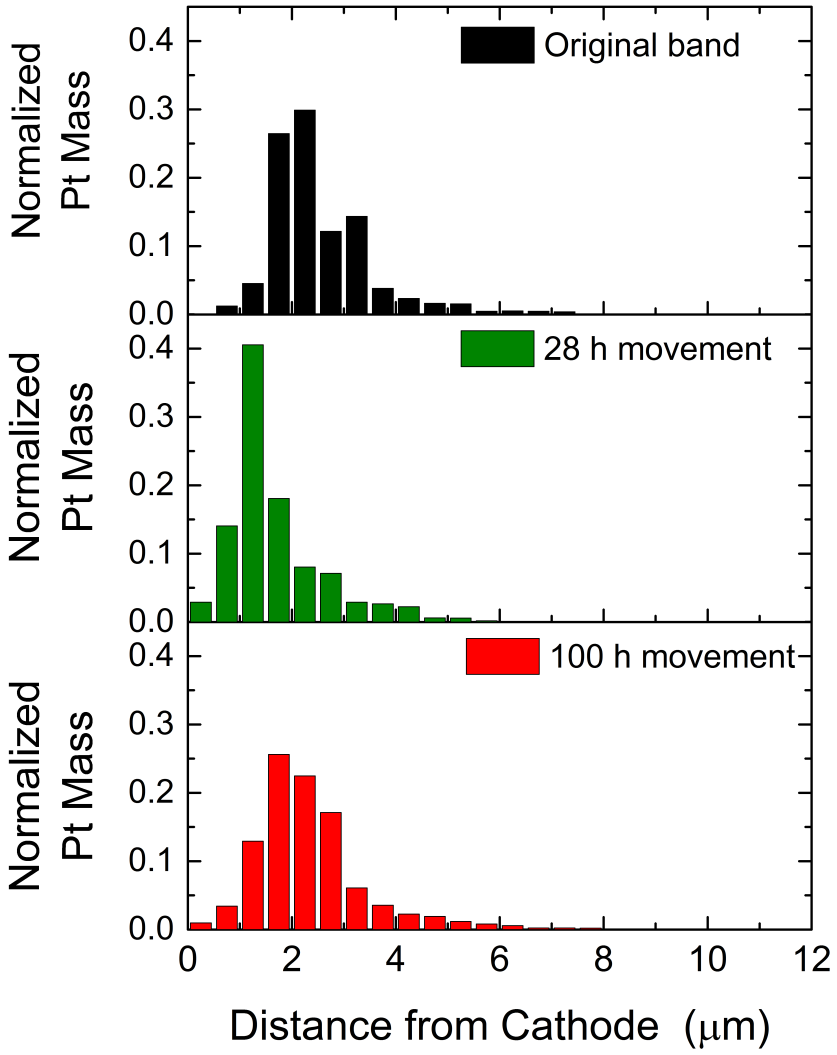


**Figure 24: Normalized Pt mass in each 0.5 μm segment of membrane. Results are averaged from multiple SEM images**

Figure 24 shows the normalized mass of the Pt bands from the baseline experiment and after the two Pt movement protocols. The previous images only contained data from a single SEM image each, while this figure includes the average normalized mass of 3 images for each experiment. Although the peaks of the mass are not perfectly aligned, this is most likely due to error in

setting the reference from which the particle distance is measured. As seen in Figure 14 and Figure 15 earlier in the chapter, the edge of the cathode CL is not always perfectly straight so there is error with this. The average distance to the CL is measured which normally varies about +/- 0.3 μm. Also, if there are large Pt particles near the edge of the 0.5 μm bins used to sum up the particles, then falling in one bin or another will significantly affect the mass in the respective bins. This is significant when the Pt particles are large, near the peak of the plots, but much less so with the small particles further from the cathode. This figure again demonstrates that there is no perceptible increase in Pt mass near 6.5 μm from the cathode, as would be expected if the Pt undergoing dissolution, migration and precipitation in the new location of the drop in Pt surface potential.

### 3.3 Double Platinum Band

An experiment was developed to test how the formation of a Pt band affects the formation of subsequent bands. This will help in the understanding of Pt band formation, but also give some insight into the effect of the existing Pt's effect on the $O_2$ crossover during the Pt movement protocols. If the second Pt band forms past the first, it is safe to assume that the Pt surface potential profile was shifted during the Pt movement protocol, despite no Pt movement being observed. For this test two 10,000 cycle ASTs, first creating a Pt band near the cathode and then increasing the $O_2$ crossover to attempt forming a second band past the first band (further from the cathode). The conditions to form each band are the same as used in previous experiments, to create a band first near 1.5 μm and then form the second band near 6.5 μm during the second 10,000 cycles. The results from this experiment are shown in Figure 25.

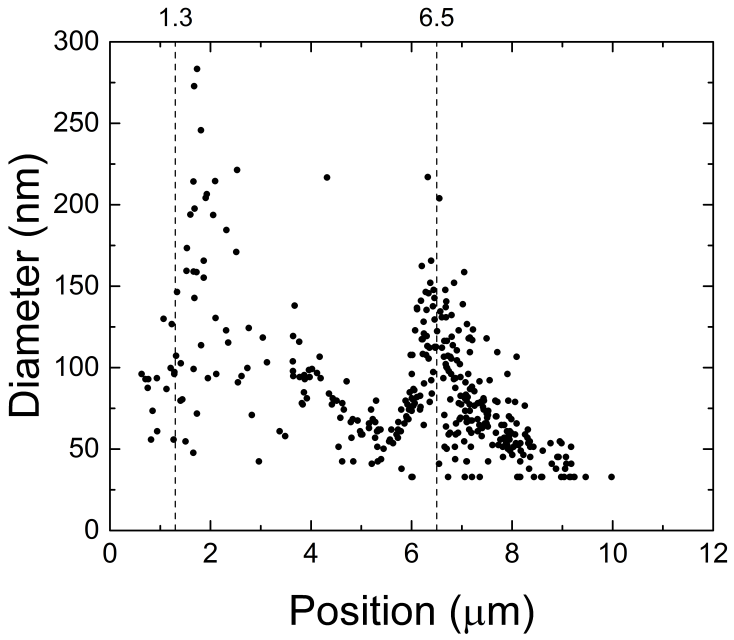


**Figure 25: Dual band experiment Pt particle data. Dotted lines represent the predicted location of band formation during the two stages of ASTs**

In Figure 25 there are clearly 2 Pt bands that have been formed. This is the first systematic and measured results to show 2 Pt bands. Kim et al. showed Pt in various positions in the membrane using TEM when 2 stages of OCV ASTs were performed [27], however they do no quantify the band in any way and they also make claims which are unsubstantiated. These bands formed where they were predicted and match the locations of the particles formed in the same locations in previous experiments. This Pt bands appear to be a superposition of experiment 1 and 2, shown in Figure 17 and Figure 18. It does not look as if Pt particles in the first band were affected in any way, nor does the position of the second band seem to have been affected by the presence of the first band. This indicates that the shift of the Pt potential profile due to increasing $O_2$ crossover was probably the same during the Pt movement protocol experiment, so the Pt was

in a high potential/$O_2$ rich environment despite no dissolution or movement being detected. The Pt in this study have traveled past the existing Pt (or any Pt ions that tried to precipitate onto existing particles were unable to due to the high potential) and proceeded to precipitate at the location where the $O_2$ and $H_2$ were in stoichiometric ratios.

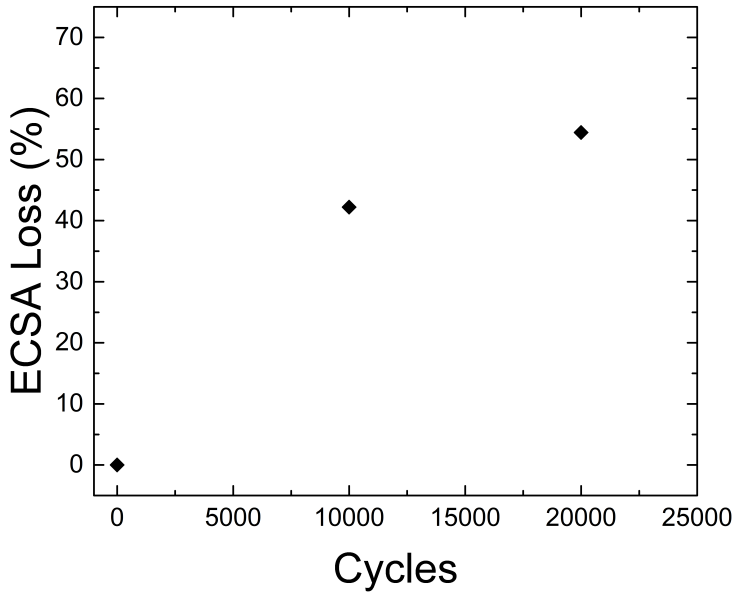


**Figure 26: ECSA loss for dual band experiment**

Looking at the ECSA loss, it shows that much more ECSA loss occurred in the first 10,000 cycles. Figure 26 shows 42% ECSA loss in the first stage, with only 14% additional loss in the second stage AST. At first this might seem to suggest that some of the Pt in the second band has to originate from the first band, and the Pt in the membrane was moved. However, the ECSA only measures the surface area of Pt in the cathode. This loss is due to both particle growth and Pt moving into the membrane. The balance between these losses is not known. Also, if the

particles in the second stage AST are larger on average, the ECSA loss when they are dissolved will be smaller for the same amount of Pt mass that is lost. This is due to the lower surface area to volume ratio with larger particles. There is some evidence of particles in the first band reacting which was not seen in any other experiment. Some particles looked as if they had been corroded with very rough edges and non-uniform shapes, though the amount of particles like this was a tiny fraction of the particles in the membrane.

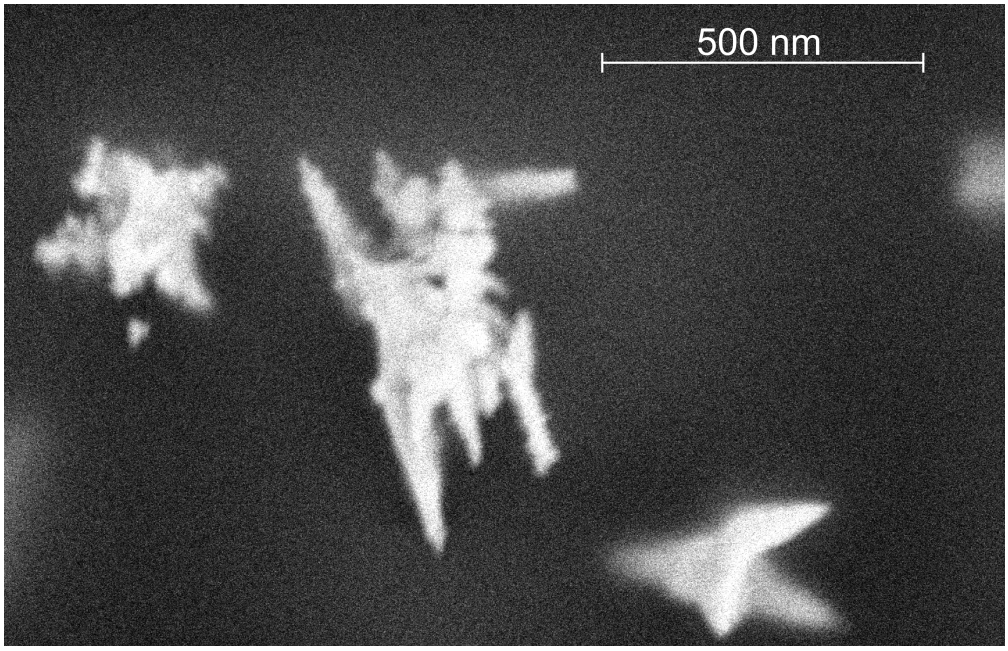


**Figure 27: SEM image of very large particles with non-smooth surfaces in the location of the first band of the dual band experiment. These particles were rare**

Figure 26 shows these rough, corroded looking Pt particles, unlike almost all others. They are non-uniform and are not close to the shape of most Pt crystals which often form cubes or stars to achieve lower surface energy and preferential growth on certain crystal faces. This suggest that there was oxidation/reduction occurring on these particles, but looking at the overall macro Pt

mass distribution and that very few of the particles appeared this way, it does not seem to have led to Pt moving from the first to second band locations.

## 3.4 Discussion

The results of the experiments were discussed somewhat, but mostly in isolated observation. The next portion of this chapter will attempt to put the results into context with the objectives and other work in the field.

### *3.4.1 Movement Discussion*

The goal of this work was to move the Pt that had precipitated in the membrane of the fuel cell, so that in future work it might be moved back to the cathode and participate in the electrochemical reactions driving the fuel cell once more. This might allow fuel cells to be brought in to be re-conditioned after extended use to improve their performance somewhat. Near the cathode the $H_2$ concentrations are low and the HOR is limited by diffusion of the $H_2$, so the ORR is the dominant reaction on the Pt surface. The particles are electrically disconnected so each particle is at OCV, with the potential for the ORR reaction at 1.23V, while the HOR potential is 0V. Although this work used potential cycling to cause the Pt dissolution in the cathode, running a cell at OCV is another common AST to cause dissolution. Some of the literature claims the Pt undergoes repeated oxidation/reduction as it moves from the cathode to its final resting place in the area which forms the Pt band due to interaction with the $O_2/H_2$ [26], [27]. The location of the band is where the HOR becomes dominant and the surface potential of the Pt drops too low to allow more dissolution; this is represented by a sharp drop in potential of the Pt surface potential profile in Figure 19. It was hypothesized that increasing the $O_2$ crossover

would shift the location of this potential drop further from the cathode, raising the surface potential of the Pt particles formed anywhere between the cathode and the potential drop. After applying the Pt movement protocols, it does not appear that the Pt is moving, or at least not at a rate which is significant over the time periods of the tests (28h and 100h).

It is suspected that the repeated oxidation/reduction as proposed by other researchers could still be occurring as the Pt moves from the CL to the band location, but it may only happen with very small and highly unstable particles. In the case of the particles in the membrane, the particles in the membrane are already very large after 10,000 potential cycles. The Pt particles when on the cathode are less than ~3nm in diameter while the particles in these bands which are counted in the SEM images are all >30nm (though there are particles smaller than this that just cannot be resolved with the settings that were used). In studies examining Pt degradation and growth in the membrane, it has been found that the smaller the particles, the more degradation occurs, measured as ECSA loss and particle growth [8]–[10]. Holby et al. suggests increasing particle sizes from the common 2-3 nm range only slightly to 4-5 nm would have significant increases in stability over PEM fuel cell time scales [11]. Particle growth has been modeled with similar results [12]. This instability they describe is due to the Gibbs-Thomson effect, which says particles with a smaller radius require increased energy to form this highly curved surface. The equation for this is:

$$E_{GT} = \frac{4\gamma\Omega}{d} \tag{1.19}$$

Where $E_{GT}$ is the increased voltage experienced on the particle due to the Gibbs-Thomson effect, $\gamma$ is the surface energy (0.148 eV/Å$^2$ for Pt), $\Omega$ is the volume per atom (15.4 Å$^3$/atom for Pt) and

d is the diameter of the particle. The energy vs particle size for a Pt particle is plotted in Figure 28. Particles in the CL are very small, below 10 nm and more like 3 nm in a fresh MEA, and experience increases in energy of these particles are several hundred millivolts. The particles in the Pt band are much larger than the particles in the CL and more stable, having almost no impact due to the Gibbs-Thompson effect, which is likely the reason why no movement occurred.

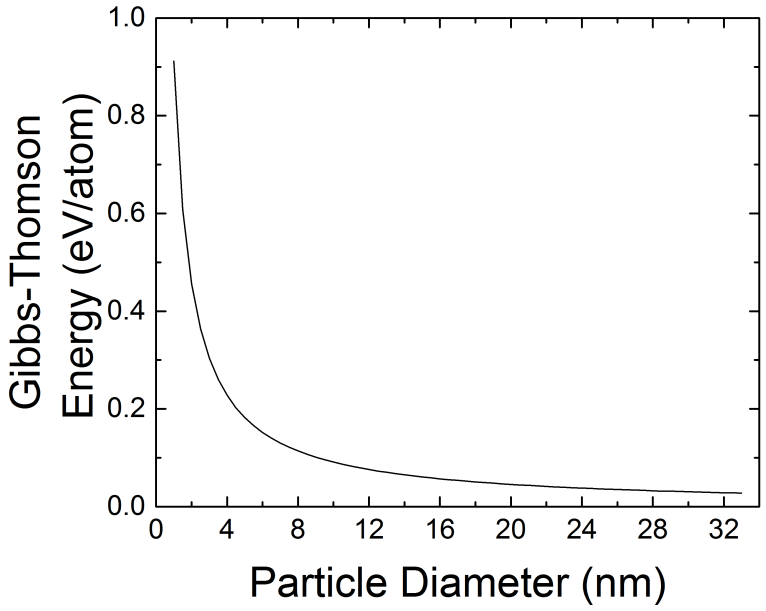


**Figure 28: Energy increase on particles vs bulk material (radius = infinity)**

Another possibility for not achieving Pt movement during the Pt movement protocol experiments was that the potential profile shown in Figure 19 did not shift as expected when the cathode BP was increased. This could be due to consumption of $O_2$ crossing the membrane when catalyzed on existing Pt particles. The lower average voltage of the cell at 0.6V would consume more $O_2$ and $H_2$, but very high stoichiometries of ~12 were used at both electrodes so that there wouldn't

be a lower concentration or diffusion of these gases. The dual Pt band experiment was developed to check that the Pt surface potential profile shifted as predicted, with the large drop in potential moving from about 1.3 to 6.5 μm. The dual band experiment resulted in a second band formed exactly where the model used predicted around 6.5 μm. This means that the presence of the Pt from the first band did not affect the potential profile, so the Pt in the movement experiments was in the high potential region despite no movement being observed. This is probably due to the high stability of these large particles as mentioned, with dissolution occurring far too slowly to be noticed during the timescales involved in this study. The formation and location of the second band also show that the Pt of the second band does not seem to be affected in any significant way. A very few number particles in the first band, as shown in Figure 27 seem to have additional reactions which caused irregular particle shapes. This was not seen in the standard movement experiments, so it must be due to the Pt formed in the second stage AST interacting with the particles. However, the overall Pt mass and particle distributions do not seem to be affected by this small amount interaction with these Pt particles.

### *3.4.2 Band Distributions*

Although it was not discussed and may not have been obvious in the previous figures, there exists a difference in the distribution and size of the particles formed in location 1 vs location 2. This has not been compared before in a quantitative way before. The bands were fitted with various functions to attempt to quantify the distribution of the particles, however the 2D nature of the data (size and diameter) made this difficult to compare. The function for fitting the bands was also unknown and no simple regression could give meaningful relationships to every Pt band; applying a normal distribution to the band formed far from the cathode gave a reasonable

relationship, but this did not fit for the near band. This also could only be applied to the particle positions, which disregards the size; or it could be applied using the normalized mass as the frequency for a given particle location, but this disregards the particle locations. Another method was developed which combines the size and particle locations.

The following figures are an attempt to display the distributions in an easier way than the basic size vs location plots used previously. The importance of the band distributions is not only for better understanding the formation of the band, but there have been studies that show Pt in the membrane can either positively or negatively influence membrane degradation/lifetime, although they are often contradictory. More recently studies by Macauley et al. (experimental), and Burlatsky & Atrazhev (modeling) have shown that low loading of small Pt particles causes fast membrane degradation, while high loading of large Pt particles mitigates membrane degradation [53], [54]. Understanding the formation of the bands and the distribution is therefore very important for membrane degradation as it may have completely opposite effects depending on the formation of the band.

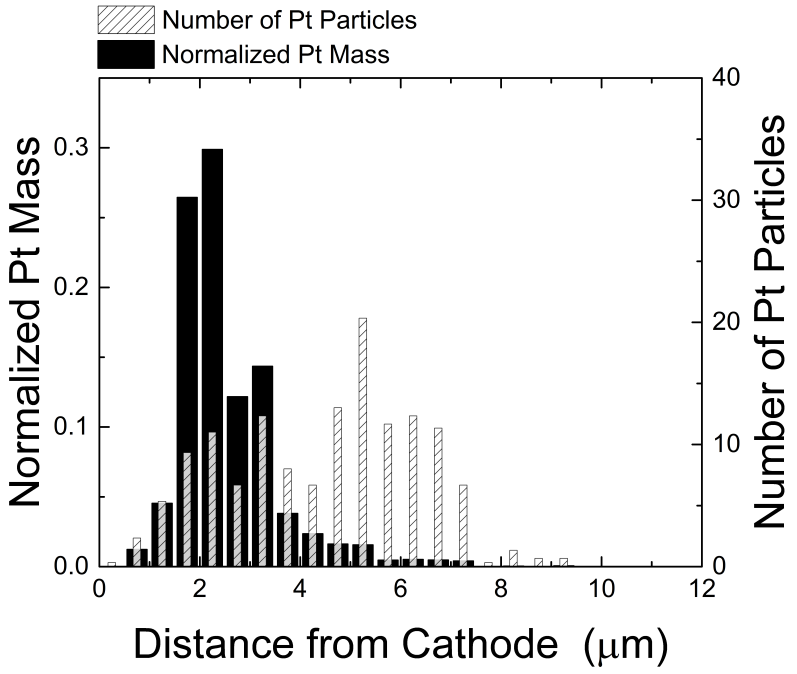


**Figure 29: Normalized Pt mass and number of particles for platinum bands formed in experiment 1 near the cathode**

Figure 29 shows the Pt band which is formed near the cathode in experiment 1. The normalized mass shows that the most mass near 2 μm from the cathode CL interface. This peak is close to the predicted location of 1.3 μm, with this offset most likely from error in estimation of the CL interface due to it not being perfectly straight in the SEM images; the standard fluctuation of CL interface was about +/-0.3μm. What is interesting when the band is view like this is distribution of the number of particles; although the majority of the mass is near 2 μm, while the majority of the particles are much further. This large number of particles represent a very little bit of mass, meaning that they are very small in size; it is not obvious in previous images with diameter vs location data that this large amount of Pt particles further from the cathode represent such a small amount of mass.

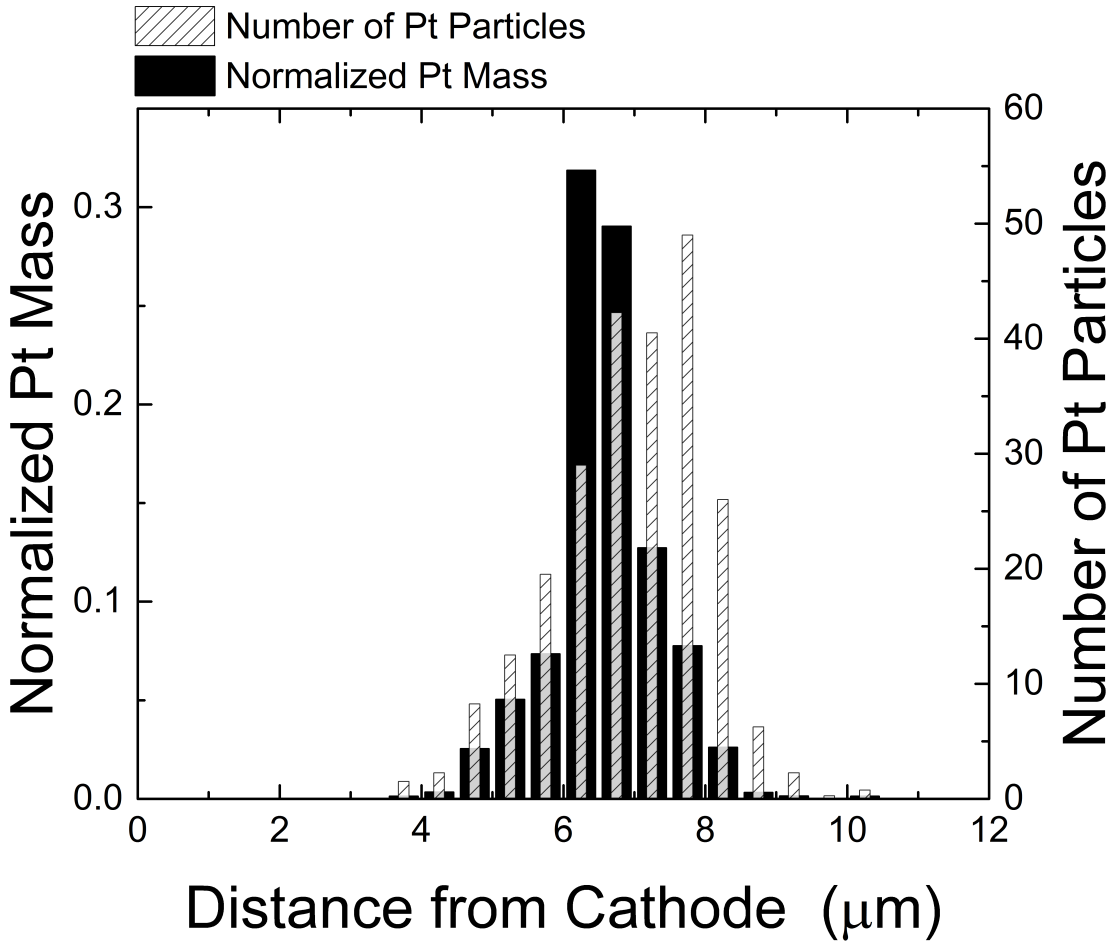


**Figure 30: Normalized Pt mass and number of particles for platinum bands formed in experiment 2, far from the cathode**

Figure 30 shows the same normalized mass and count vs location, but for the band formed in experiment 2. The mass is centered on 6.5 μm as predicted. Unlike the band formed near the cathode in Figure 29, the mass and number of Pt particles are more overlapped. The large amount of mass is made up of more particles, meaning that the average particle size is smaller. The distribution of particle sizes is also not as wide which is more obvious when the average particle size is calculated by dividing the mass by the number of particles, then calculating the diameter from this average particle mass. The results are shown in Figure 32.

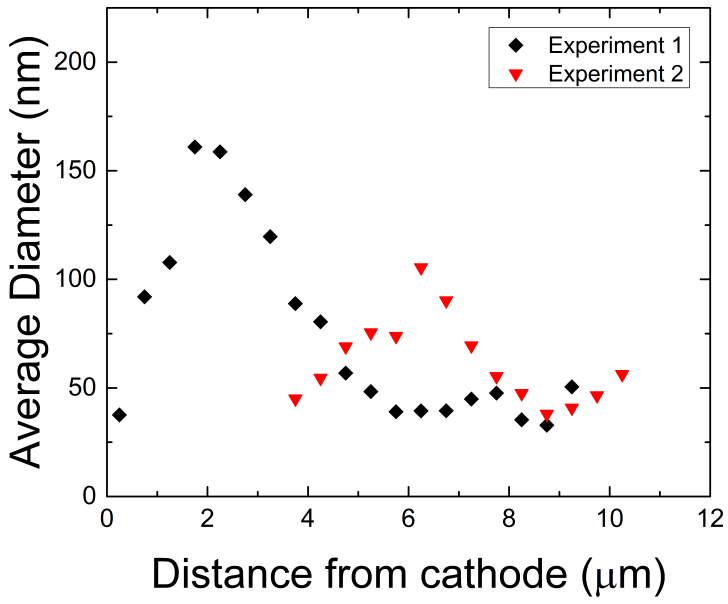


**Figure 31: Average Pt particle diameter derived from average mass**

The average particle size derived from average particle mass is displayed in Figure 31. This is an easy comparison of the size of particles. The maximum average Pt particle diameter of experiment 2 is 105 nm while the max size for experiment 1 is 161 nm and increase almost 53%. Comparing the average masses of these same tests at their peaks is a difference of 255%. This demonstrates how much more concentrated the mass is in the band nearer the cathode, while the band that is further is more evenly distributed (though the overall range of particles is not as wide.

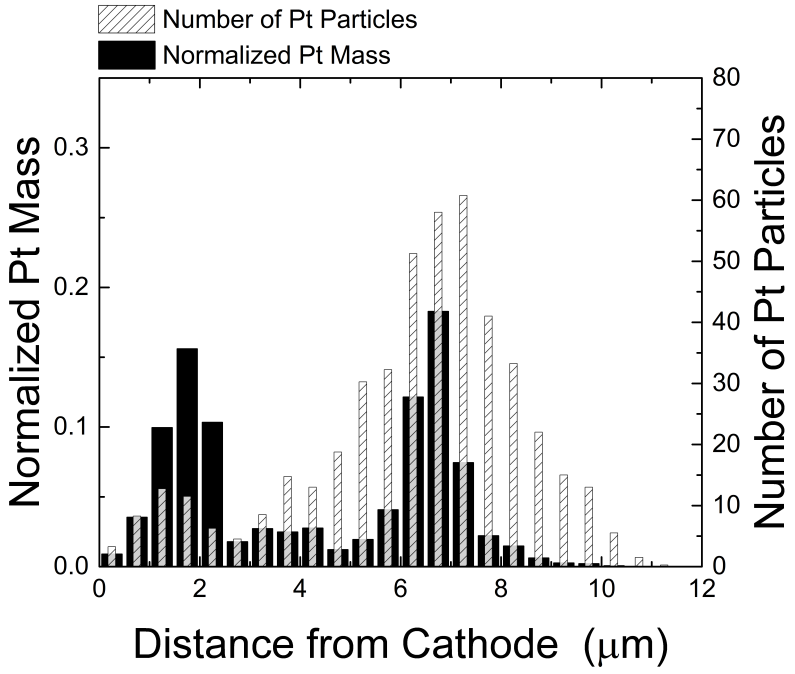


**Figure 32: Normalized Pt mass and number of particles for platinum bands formed in the 2 stage AST experiment**

Figure 32 shows the distribution of mass and particles of the dual band experiment. As mentioned before, this appears to be a superposition of experiment 1 and 2, in terms of both mass and particles. There are two large accumulations of mass in the locations the band, as well as an increasing number of particles as distance increase from the cathode up until the second band location and then tapering down. It is the same as the previous examples in that the band near the cathode is made up of much fewer and larger particles, while the second band is made up of many more smaller particles. This is obvious again when the average Pt particle diameter is calculated. This is plotted in Figure 33.

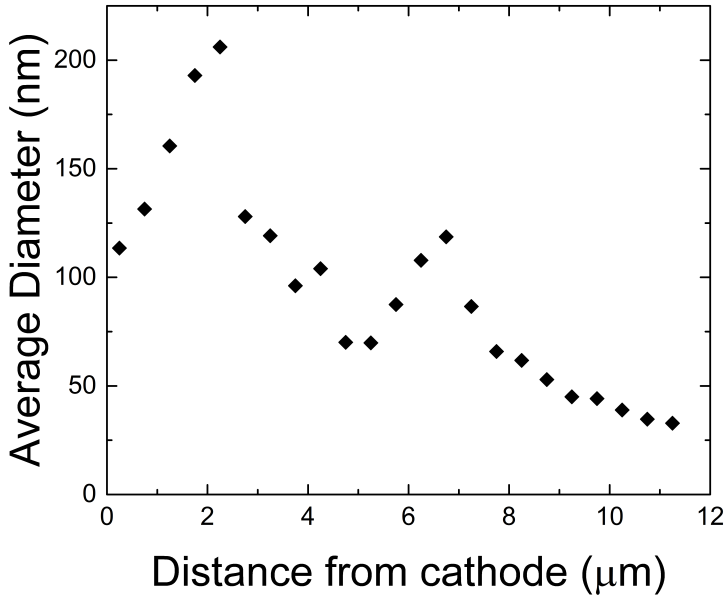


**Figure 33: Average Pt particle diameter derived from the average mass of the dual band experiment**

Figure 33 displays the average particle diameter as derived from the average mass from the dual band experiment. The largest particles in the peak near the cathode are much larger than those in the second band. The larges particles in the left peak are 206 nm while the smaller peak particles are only 118, a difference of 75% in diameter or 432% in mass. However, when the overall mass of the two bands are compared as in Figure 32, the mass of the peak of the second band is actually slightly higher because there are so many more particles in this area.

The importance of the band distributions is in understanding the Pt formation in the membrane, but also in regards to membrane degradation. From the figures it is observed that the Pt band is not always formed the same way in different locations within the membrane. The particles in the

band near the cathode are not evenly distributed; the particles do not nucleate and then grow evenly throughout the membrane. Near the cathode there are very few particles that make up the majority of the Pt mass in the membrane due to the size being so much larger than the other particles in the membrane. In the band formed further from the cathode, the larger particles are also the more numerous. The dual band experiment appears to be a super position of these two situations, with large peaks in mass in the same locations, but the most Pt particles at the point where the second band forms. This is very interesting regarding the relationship between Pt nucleation and growth, and how it is so much different for the two band locations. It seems as if the critical radius is not the same in the different band locations, with the critical radius being larger nearer the cathode, which is why there are fewer larger particles. This may be due to the Pt surface potential profile being different for different gas crossovers, though the relationship would need to be connected to a model or study where they measured this profile [30]–[33]. These studies do not really seem to show much difference in shape of the profile, just the location of the potential drop region. Another influence may be the expanded EPTFE layer in the center of this membrane, which was not considered in the modeling papers. This layer may affect both the transport of the gases, or the Pt movement in a way that influences the band which forms close to this layer differently than the band formed away from the layer, however this would probably result in the band formed near the layer to be skewed in some way, and this band is much more symmetric than the band formed near the cathode. A separate test showed that Pt can still form in the band, and the band looked similar to the band that was formed farther from the cathode. SEM images for this test are in the Appendix.

Although the cause of the differing distributions is still unknown, the distributions themselves may be significant in regards to membrane degradation. Rodgers et al. shows how the membrane degradation rate is different with the various Pt concentrations they impregnated the membrane with [50]. Other researchers show cases of Pt increasing [48], or decreasing membrane degradation rates [51]. Although inconsistent, all of these results show that there may be a very subtle but extremely important relationship between the Pt size and distribution, and the resulting degradation of the membrane. Burlatsky & Atrazhev have recently used a model with the results that low loading of small particles speed up membrane degradation, while high loading of large particles mitigates degradation [53]. Understanding and knowing the distribution of the band that will be formed in the membrane may be more important than just being aware that a band exists, as was previously thought. There may even be a different effect on the degradation of the membranes when Pt bands are formed in different locations in the same membrane because they may have different distributions as shown here. In this case, knowing which operating pressures lead to which type of band formation could be adjusted to ensure longer lasting membranes. Tuning precipitation models like Burlatsky et al.'s [23], with more accurate characterization of the Pt band and combining this with membrane degradation modelling could be very powerful in predicting lifetimes of membranes.

### *3.4.3 Platinum Mass Balance*

Although the Pt in the membrane has been measured throughout this work, the comparisons have all been made by normalizing the Pt mass. The mass of Pt is the important parameter for the Pt in the membrane, because this is the amount of Pt that has been lost from the CL (though surface area in the CL is more important as this is what impacts the performance of the cell).

Unfortunately the methods that have been used with the SEM, although the mass of individual particles can be estimated, the overall Pt in the membrane is a difficult quantity to determine. This is because the control volume for the images is unknown. The width and height of each images is known, but the depth at which the electrons penetrate the membrane and exit to produce a signal needs to be known so that a density of Pt can be calculated for each image. Extrapolating for the entire volume of the membrane in the cell would then give the total Pt mass lost from the cathode CL. TEM samples have the advantage that the thickness of the sample can be measured, and since the electrons pass through the entire sample, the control volume can be calculated. The depth of BSE in a sample can be estimated for an elemental material using the equation:

$$R = \frac{0.0276A}{Z^{0.89}\rho} E_0^{1.67} \tag{1.20}$$

Where R is the depth of the electrons in μm, A is the atomic mass in g/mol, $E_0$ is the accelerating voltage in keV, Z is the atomic number and ρ is the density of the material in g/cm$^3$. This equation is cannot be directly used for the membrane because there is not an atomic number for a polymer, however, using the equation for carbon the depth of electrons is 0.43 μm. The density of Nafion is roughly similar to carbon, so this may give a reasonable range for the depth of electrons in the sample. The depth of the electrons is very important, and to illustrate this, a plot of the estimated total Pt mass in the membrane is plotted vs different depths.

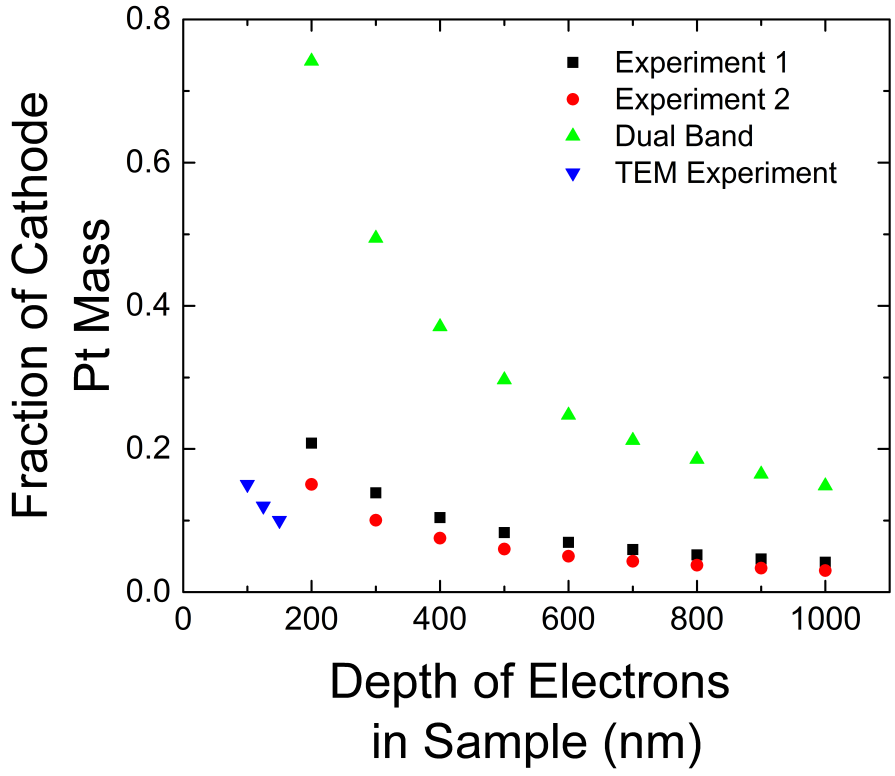


**Figure 34: Estimated Pt mass in the membrane as fraction of the initial Pt mass in the cathode CL, depending on the depth of electron penetration**

Figure 34 demonstrates the estimated mass of the Pt in the membrane as a fraction of the Pt mass initially in the cathode CL base on the manufacturer's 0.4 mg/cm$^2$ loading. If the depth of the electrons is less, the density of the Pt in an image is higher, leading to a larger overall mass. The estimated depth of 0.43 μm seems reasonable for experiment 1 and 2 when compared to the mass calculated from a TEM image (also plotted on in Figure 34). Unfortunately the thickness of the TEM sample was not measured, but the thickness of these samples is on the order of 100-200 nm. If the ECSA from the experiment from which the TEM image was taken is compared to

experiment 1 and 2, it has approximately 1.6x the ECSA loss. This is shown in Figure 35. The estimated Pt mass in the membrane using an electron penetration of 400 +/- 100 nm could be reasonable as at this range the Pt mass in the membrane as shown by the TEM image is roughly 1.6x greater than for experiment 1 and 2. These estimates however are questionable when looking at the dual band experiment. The dual band experiment is expected to have roughly the same Pt mass as the sum of the mass in experiment 1 and 2, as the experiment was both of these experiments together. But when looking at the plot in Figure 34 the mass in the dual band experiment is much more than the sum of the other two. This may be due to the impact of how well the SEM was focused for each experiment. If the focus was slightly out of plane, especially if the focal plane was above the plane of the sample, this would show less Pt in the images.

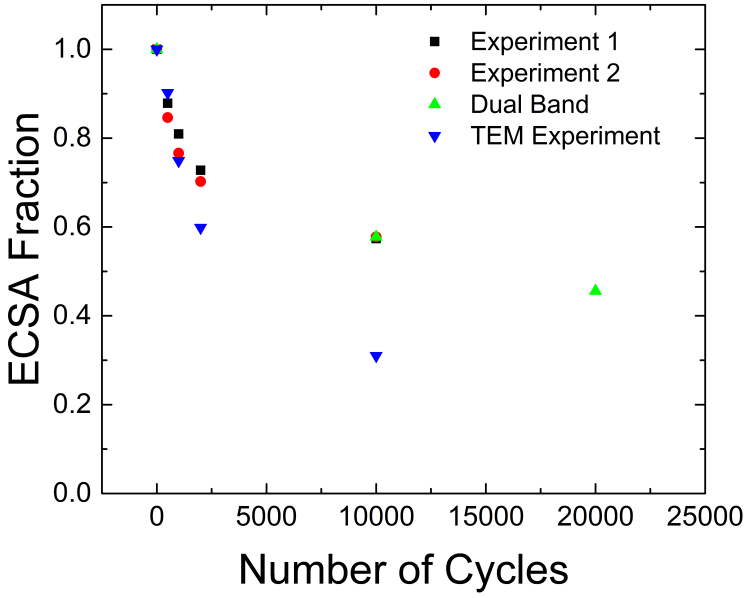


**Figure 35: ECSA comparison of experiments plotted in Figure 34**

When looking at Figure 35, it shows that the rate of decrease in ECSA slows as the number of cycles increases. This is due to the increase in particle diameter due to Ostwald ripening, which increases the stability and decreases the dissolution rate of the particles. At 10,000 cycles 3 of the experiments have the same ECSA, but the estimated Pt mass in the membrane shown in Figure 34 is different. For experiment 1 and 2 the difference could be that there is a higher $H_2$ crossover in experiment 1, which has been said to increase the concentration gradient of Pt ions in the membrane and therefore increase diffusion into the membrane [16]. For the dual band, the mass in Figure 34 is after 20,000 cycles, but is more than the sum of experiment 1 and 2, which is what it is expected to be. Comparing the loss in ECSA of the dual band experiment from 10,000 to 20,000 cycles, the loss only increase by ~10% in the second 10,000 cycles. It is possible to have a similar loss of mass in both stages (shown in Figure 32) while only having a small loss of surface area if a lot of the loss was due to Ostwald ripening and because the particles in the second stage are larger, so any mass loss represents a smaller surface area loss (due to scaling effects). It seems like the large difference in mass from the dual band to experiment 1 and 2 is likely due to a difference in focal planes in the images because of how different the estimated masses are, but from this data it is estimated that 5% to 40% of the Pt mass in the cathode has moved into the membrane depending on the experiment. In the future, TEM images with measured sample thicknesses would aid in getting a much more accurate estimation of Pt mass lost to the membrane.

## Chapter 4: Conclusion

The precipitation of Pt in the membranes of PEM fuel cells after extended use is a real issue. This Pt represents lost catalyst surface area from the cathode which leads to reduced performance of the cell. If Pt that is precipitated in the membrane could be re-dissolved and moved, it is possible that this Pt might be returned to the cathode and be reactivated. A set of experiments was designed to create Pt bands, and try and more these bands. This work applied new quantitative methods to existing SEM techniques in an attempt to better understand the formation of the Pt band as well as any Pt movement. Characterizing the Pt band better is also important for Pt degradation studies as the Pt in the membrane can catalyze unwanted reactions. These reactions can result in radicals being formed, which leads to degradation of the membrane, or they can quench these same radicals which leads to improved membrane lifetime. The interplay between forming and quenching radicals is still being researched but it seems that the differences in Pt precipitation leading to each one are subtle.

The main results and takeaways from this work can be summarized as:

- Platinum bands were made in two distinct and predicted locations (using existing model)
- Applying new quantitative image analysis developed in this work, these bands were found to be different in their size and distribution of Pt particles. This is significant for understanding Pt precipitation in the membrane, and is also important for membrane degradation studies trying to understand the effects of the Pt band

- A platinum movement protocol was developed to use $O_2$ to cause dissolution and movement of Pt in the membrane. No Pt movement was observed over the timeframes studied (28h and 100h). This is most likely due to the high stability of large particles
- Dual Pt bands were formed. This work was the first to quantify this. The location of the second band was not affected by the presence of the first band and was formed in the predicted location
- The dual Pt bands were a superposition of the two individual bands. This applies to both the mass and particle distributions. This shows that the nucleation and growth mechanisms were also not affected by the presence of the first Pt band

Stepping back and looking at the implications of the results in this work there are several important conclusions that should be expanded upon. The first is that image analysis can be a powerful tool to get more detailed information on the Pt band. This is important for modelers and to better understand the Pt in the membrane mechanisms, as quantitative information is needed. Another important conclusion is that these results it seems that the size of the Pt particle is a very important parameter, which is most likely due to the Gibbs-Thomson effect raising the potential of the smaller particles. The small Pt particles in the CL are prone to dissolution, while the large particles in the membrane seem to be extremely stable over same timeframes. This means that if it were possible to cause dissolution of the Pt in the membrane in the hopes of moving the Pt, it would need to be done to very small particles, or it would take much too long to be practical for reconditioning a damaged cell. It is unlikely that it would be possible to keep the Pt in the membrane small enough for this as the growth rate of the particles (especially in the band nearer the cathode) is much higher than the nucleation rate. This means that the best strategy for

returning the Pt to the cathode CL is to never let the Pt leave the cathode in the first place. This may be achieved partially by the operational parameters of the cell, but most likely will need improved material characteristics for the CL. The Pt precipitation is also a very interesting and important result. The Pt band near the cathode had larger but less numerous particles than the Pt band further from the cathode. This shows that nucleation rate is lower near the cathode, but the particles have a higher growth rate. The causes for this are unknown, but it must be to different local environments in the two locations. Understanding the differences is important as the differences in the Pt bands is important for membrane degradation. If these bands cause different membrane degradation, then the operating conditions of the cell could be very important for ensuring a long cell lifetime. The last important result from this work is that when the dual bands were formed, the location, nucleation rate and growth rate of the second band that was formed seemed to be independent of the presence of the first band. This shows that the Pt in the membrane does not seem to influence the gas crossover or other conditions that effect the Pt band precipitation. The two bands were also the same as the bands formed in the individual experiments, backing up the difference in nucleation and growth differences in the two locations in the membrane. All of these results are important as PEM fuel cells attempt to enter the commercial market and degradation/lifecycle testing is important in creating durable and reliable fuel cells. There needs to be a lot more work before these mechanisms are fully understood, but the use of image analysis will be important for this moving forward.

## 4.1 Recommendations

The quantitative characterization that was developed in this work is a next step in understanding Pt band formation and Pt precipitation. The characterization shows how much variation the mass

and particle distributions have, as well as how bands formed in different spots have different mass and particle distributions from each other. Although previous studies may have mentioned different sizes of particles, modelling requires numerical information; Pt band models should be able to use the information to developed improved models. A logical next step for this work is to measure the precipitation and development of the band over time. Experiments for this have been started, but are not complete. Other studies examining Pt bands should attempt to use similar techniques to better characterize their Pt bands to gather more information than has been in the past, whether using SEM, TEM or another morphological technique. The distributions of Pt are also important for studies exploring membrane degradation. They are just beginning to understand when Pt causes more degradation of helps to mitigate degradation. Applying characterization like this while measuring membrane degradation should help to further improve this understanding, knowing which Pt distributions lead to what level of degradation. Lastly, since the bands formed in this work are different and may lead to different membrane degradation rates, setting operation parameters in fuel cells which lead to the formation of Pt bands with more favorable effects on membrane degradation will lead to extended lifetime for the membrane in real operations.

## References


[1] The Intergovernmental Panel on Climate Change (IPCC)., *Climate Change 2014: Mitigation of Climate Change*. 2014.

[2] Environment Canada, "Greenhouse Gas Emissions by Economic Sector," *Government of Canada*, 2014. [Online]. Available: http://ec.gc.ca/indicateurs-indicators/default.asp?lang=en&n=F60DB708-1. [Accessed: 12-Feb-2016].

[3] S. Zhang, X.-Z. Yuan, J. N. C. Hin, H. Wang, K. A. Friedrich, and M. Schulze, "A review of platinum-based catalyst layer degradation in proton exchange membrane fuel cells," *J. Power Sources*, vol. 194, no. 2, pp. 588–600, Dec. 2009.

[4] M. S. Wilson and S. Gottesfeld, "Thin-film catalyst layers for polymer electrolyte fuel cell electrodes," *J. Appl. Electrochem.*, vol. 22, no. 1, pp. 1–7, 1992.

[5] E. C. S. Transactions and T. E. Society, "Characterization and Performance of Catalyst Layers Prepared By Inkjet Printing Technology Madhu S. Saha," vol. 58, no. 1, pp. 797–806, 2013.

[6] O. A. Uchida Makoto, Fukuoka Yuko, Sugawara Yasushi, Ohara Hideo, "Improved Preparation Process of Very-Low-Platinum-Loading Electrodes for Polymer Electrolyte Fuel Cells," *J. Electrochem. Soc.*, vol. 145, no. 11, pp. 3708–3713, 1998.

[7] R. O'Hayre, S. J. Lee, S. W. Cha, and F. B. Prinz, "A sharp peak in the performance of sputtered platinum fuel cells at ultra-low platinum loading," *J. Power Sources*, vol. 109, no. 2, pp. 483–493, 2002.

[8] R. K. Ahluwalia, S. Arisetty, J.-K. Peng, R. Subbaraman, X. Wang, N. Kariuki, D. J. Myers, R. Mukundan, R. Borup, and O. Polevaya, "Dynamics of Particle Growth and Electrochemical Surface Area Loss due to Platinum Dissolution," *J. Electrochem. Soc.*, vol. 161, no. 3, pp. F291–F304, 2014.

[9] P. J. Ferreira, G. J. la O', Y. Shao-Horn, D. Morgan, R. Makharia, S. Kocha, and H. a. Gasteiger, "Instability of Pt/C Electrocatalysts in Proton Exchange Membrane Fuel Cells," *J. Electrochem. Soc.*, vol. 152, no. 11, p. A2256, 2005.

[10] Z. Yang, S. Ball, D. Condit, and M. Gummalla, "Systematic Study on the Impact of Pt Particle Size and Operating Conditions on PEMFC Cathode Catalyst Durability," *J. Electrochem. Soc.*, vol. 158, no. 11, pp. B1439–B1445, 2011.

[11] E. F. Holby, W. Sheng, Y. Shao-Horn, and D. Morgan, “Pt nanoparticle stability in PEM fuel cells: influence of particle size distribution and crossover hydrogen,” *Energy Environ. Sci.*, vol. 2, p. 865, 2009.

[12] F. Hiraoka, Y. Kohno, and K. Matsuzawa, “A Simulation Study of Pt Particle Degradation During Potential Cycling Using a Dissolution / Deposition Model,” pp. 102–108, 2015.

[13] M. S. Wilson, “Surface Area Loss of Supported Platinum in Polymer Electrolyte Fuel Cells,” *J. Electrochem. Soc.*, vol. 140, no. 10, p. 2872, 1993.

[14] Y. Shao-Horn, W. C. Sheng, S. Chen, P. J. Ferreira, E. F. Holby, and D. Morgan, “Instability of Supported Platinum Nanoparticles in Low-Temperature Fuel Cells,” *Top. Catal.*, vol. 46, no. 3–4, pp. 285–305, Nov. 2007.

[15] M. Zhao, W. Shi, B. Wu, and W. Liu, “Analysis of carbon-supported platinum through potential cycling and potential-static holding,” *Int. J. Hydrogen Energy*, vol. 39, no. 25, pp. 13725–13737, 2014.

[16] E. F. Holby and D. Morgan, “Application of Pt Nanoparticle Dissolution and Oxidation Modeling to Understanding Degradation in PEM Fuel Cells,” *J. Electrochem. Soc.*, vol. 159, no. 5, p. B578, 2012.

[17] T. T. H. Cheng, E. Rogers, A. P. Young, S. Ye, V. Colbow, and S. Wessel, “Effects of crossover hydrogen on platinum dissolution and agglomeration,” *J. Power Sources*, vol. 196, no. 19, pp. 7985–7988, Oct. 2011.

[18] K. Yu, D. J. Groom, X. Wang, Z. Yang, M. Gummalla, S. C. Ball, D. J. Myers, and P. J. Ferreira, “Degradation Mechanisms of Platinum Nanoparticle Catalysts in Proton Exchange Membrane Fuel Cells: The Role of Particle Size,” 2014.

[19] T. Patterson, “Fuel cell technology topical conference proceedings,” *AIChE Spring Natl. Meet. New York*, vol. 313, 2002.

[20] R. M. Darling and J. P. Meyers, “Kinetic Model of Platinum Dissolution in PEMFCs,” *J. Electrochem. Soc.*, vol. 150, no. 11, p. A1523, 2003.

[21] E. Guilminot, A. Corcella, F. Charlot, F. Maillard, and M. Chatenet, “Detection of Ptz+ Ions and Pt Nanoparticles Inside the Membrane of a Used PEMFC,” *J. Electrochem. Soc.*, vol. 154, no. 1, p. B96, 2007.

[22] V. Berejnov, Z. Martin, M. West, S. Kundu, D. Bessarabov, J. Stumper, D. Susac, and A.

P. Hitchcock, “Probing platinum degradation in polymer electrolyte membrane fuel cells by synchrotron X-ray microscopy,” *Phys. Chem. Chem. Phys.*, vol. 14, p. 4835, 2012.

[23] S. F. Burlatsky, M. Gummalla, V. V. Atrazhev, D. V. Dmitriev, N. Y. Kuzminyh, and N. S. Erikhman, “The Dynamics of Platinum Precipitation in an Ion Exchange Membrane,” *J. Electrochem. Soc.*, vol. 158, no. 3, p. B322, 2011.

[24] T. Akita, A. Taniguchi, J. Maekawa, Z. Siroma, K. Tanaka, M. Kohyama, and K. Yasuda, “Analytical TEM study of Pt particle deposition in the proton-exchange membrane of a membrane-electrode-assembly,” *J. Power Sources*, vol. 159, pp. 461–467, 2006.

[25] K. Yasuda, A. Taniguchi, T. Akita, T. Ioroi, and Z. Siroma, “Platinum dissolution and deposition in the polymer electrolyte membrane of a PEM fuel cell as studied by potential cycling.,” *Phys. Chem. Chem. Phys.*, vol. 8, no. 6, pp. 746–52, Feb. 2006.

[26] S. R. Dhanushkodi, S. Kundu, M. W. Fowler, and M. D. Pritzker, “Study of the effect of temperature on Pt dissolution in polymer electrolyte membrane fuel cells via accelerated stress tests,” *J. Power Sources*, vol. 245, pp. 1035–1045, 2014.

[27] L. Kim, C. G. Chung, Y. W. Sung, and J. S. Chung, “Dissolution and migration of platinum after long-term operation of a polymer electrolyte fuel cell under various conditions,” *J. Power Sources*, vol. 183, no. 2, pp. 524–532, Sep. 2008.

[28] J. Zhang, B. a. Litteer, W. Gu, H. Liu, and H. a. Gasteiger, “Effect of Hydrogen and Oxygen Partial Pressure on Pt Precipitation within the Membrane of PEMFCs,” *J. Electrochem. Soc.*, vol. 154, no. 10, p. B1006, 2007.

[29] W. Bi, G. E. Gray, and T. F. Fuller, “PEM Fuel Cell Pt/C Dissolution and Deposition in Nafion Electrolyte,” *Electrochem. Solid-State Lett.*, vol. 10, no. 5, p. B101, 2007.

[30] W. Liu and D. Zuckerbrod, “In Situ Detection of Hydrogen Peroxide in PEM Fuel Cells,” *J. Electrochem. Soc.*, vol. 152, p. A1165, 2005.

[31] M. Ohishi, Y. Okano, Y. Ono, A. Ohma, K. Fushinobu, and K. Okazaki, “Investigation of potential profile in electrolyte membrane of PEFC by using microprobe technique,” *Int. J. Heat Mass Transf.*, vol. 55, no. 23–24, pp. 7213–7217, 2012.

[32] V. V. Atrazhev, N. S. Erikhman, and S. F. Burlatsky, “The potential of catalytic particle in ion exchange membrane,” *J. Electroanal. Chem.*, vol. 601, pp. 251–259, 2007.

[33] M. J. Eslamibidgoli, P.-É. A. Melchy, and M. H. Eikerling, “Modeling the local potential

at Pt nanoparticles in polymer electrolyte membranes," *Phys. Chem. Chem. Phys.*, pp. 27–29, 2015.

[34] J. Peron, Y. Nedellec, D. Jones, and J. Roziere, "The effect of dissolution, migration and precipitation of platinum in Nafion®-based membrane electrode assemblies during fuel cell operation at high potential," *J. Power Sources*, vol. 185, no. 2, pp. 1209–1217, Dec. 2008.

[35] S. Kundu, M. Cimenti, S. Lee, and D. Bessarabov, "Fingerprint of automotive fuel cell cathode catalyst degradation: Pt band in PEMs," *Membr. Technol.*, vol. 2009, no. 10, pp. 7–10, Oct. 2009.

[36] F. Ettingshausen, J. Kleemann, M. Michel, M. Quintus, H. Fuess, and C. Roth, "Spatially resolved degradation effects in membrane-electrode-assemblies of vehicle aged polymer electrolyte membrane fuel cell stacks," *J. Power Sources*, vol. 194, pp. 899–907, 2009.

[37] F. Ettingshausen, J. Kleemann, a. Marcu, G. Toth, H. Fuess, and C. Roth, "Dissolution and Migration of Platinum in PEMFCs Investigated for Start/Stop Cycling and High Potential Degradation," *Fuel Cells*, vol. 11, no. 2, pp. 238–245, Apr. 2011.

[38] C. G. Chung, L. Kim, Y. W. Sung, J. Lee, and J. S. Chung, "Degradation mechanism of electrocatalyst during long-term operation of PEMFC," *Int. J. Hydrogen Energy*, vol. 34, no. 21, pp. 8974–8981, 2009.

[39] H. Schulenburg, B. Schwanitz, J. Krbanjevic, N. Linse, G. G. Scherer, and a. Wokaun, "Quantification of platinum deposition in polymer electrolyte fuel cell membranes," *Electrochem. commun.*, vol. 13, no. 9, pp. 921–923, Sep. 2011.

[40] N. J. C. Ingle, a. Sode, I. Martens, E. Gyenge, D. P. Wilkinson, and D. Bizzotto, "Synthesis and characterization of diverse Pt nanostructures in nafion," *Langmuir*, vol. 30, pp. 1871–1879, 2014.

[41] M. P. Rodgers, R. P. Brooker, N. Mohajeri, L. J. Bonville, H. R. Kunz, D. K. Slattery, and J. M. Fenton, "Comparison of Proton Exchange Membranes Degradation Rates between Accelerated and Performance Tests," *J. Electrochem. Soc.*, vol. 159, no. 7, pp. F338–F352, Jan. 2012.

[42] D. C. Johnson, D. T. Napp, and S. Bruckenstein, "A Ring-Disk Electrode Study of the Current/Potential Behaviour of Platinum Sulphuric and 0.1 M Perchloric Acids,"

*Electrochim. Acta*, vol. 15, no. January 1969, 1970.

[43] L. Xing, M. A. Hossain, M. Tian, D. Beauchemin, K. T. Adjemian, and G. Jerkiewicz, "Platinum Electro-dissolution in Acidic Media upon Potential Cycling," *Electrocatalysis*, vol. 5, pp. 96–112, 2014.

[44] X. Wang, R. Kumar, and D. J. Myers, "Effect of Voltage on Platinum Dissolution," *Electrochem. Solid-State Lett.*, vol. 9, no. 5, p. A225, 2006.

[45] M. Uchimura and S. S. Kocha, "The Impact of Cycle Profile on PEMFC Durability," *ECS Trans.*, vol. 11, no. 1, pp. 1215–1226, 2007.

[46] R. M. Darling and J. P. Meyers, "Mathematical Model of Platinum Movement in PEM Fuel Cells," *J. Electrochem. Soc.*, vol. 152, p. A242, 2005.

[47] R. L. Borup, J. R. Davey, F. H. Garzon, D. L. Wood, and M. A. Inbody, "PEM fuel cell electrocatalyst durability measurements," *J. Power Sources*, vol. 163, no. 1, pp. 76–81, Dec. 2006.

[48] S. Helmly, R. Hiesgen, T. Morawietz, X.-Z. Yuan, H. Wang, and K. Andreas Friedrich, "Microscopic Investigation of Platinum Deposition in PEMFC Cross-Sections Using AFM and SEM," *J. Electrochem. Soc.*, vol. 160, no. 6, pp. F687–F697, Apr. 2013.

[49] S. Helmly, B. Ohnmacht, P. Gazdzicki, R. Hiesgen, E. Gulzow, and K. a. Friedrich, "Influence of the Distribution of Platinum Deposits on the Properties and Degradation of Platinum-Impregnated Nafion Membranes," *J. Electrochem. Soc.*, vol. 161, no. 14, pp. F1416–F1426, Oct. 2014.

[50] M. P. Rodgers, B. P. Pearman, L. J. Bonville, D. a. Cullen, N. Mohajeri, and D. K. Slattery, "Evaluation of the Effect of Impregnated Platinum on PFSA Degradation for PEM Fuel Cells," *J. Electrochem. Soc.*, vol. 160, no. 10, pp. F1123–F1128, Aug. 2013.

[51] N. Macauley, L. Ghassemzadeh, C. Lim, M. Watson, J. Kolodziej, M. Lauritzen, S. Holdcroft, and E. Kjeang, "Pt Band Formation Enhances the Stability of Fuel Cell Membranes," *ECS Electrochem. Lett.*, vol. 2, no. 4, pp. F33–F35, Feb. 2013.

[52] N. Macauley, a. S. Alavijeh, M. Watson, J. Kolodziej, M. Lauritzen, S. Knights, G. Wang, and E. Kjeang, "Accelerated Membrane Durability Testing of Heavy Duty Fuel Cells," *J. Electrochem. Soc.*, vol. 162, no. 1, pp. F98–F107, Nov. 2015.

[53] S. F. Burlatsky and V. V. Atrazhev, "Modeling the Effect of Pt Precipitation on PEM

Degradation," *ECS Meet. Abstr.*, 2015.

[54] N. Macauley, K. H. Wong, M. Watson, and E. Kjeang, "Favorable effect of in-situ generated platinum in the membrane on fuel cell membrane durability," *J. Power Sources*, vol. 299, pp. 139–148, 2015.

[55] S. R. Dhanushkodi, M. Schwager, and D. Todd, "PEMFC Durability : Spatially Resolved Pt Dissolution in a Single Cell," vol. 161, no. 12, 2014.

# Appendices

## Appendix A

### A.1 EPTFE Effect

Another experiment was performed to see what happened to band formed in the EPTFE layer in the middle of the membrane. This is a structural support within the membrane which has slightly different chemistry from the membrane on either side of it. The results of this experiment are shown in Figure 36 and Figure 37. The edge of the EPTFE layer is about 7.3 μm away from the cathode in this experiment and continues to about 15 μm away from the cathode, so the majority of the band is within this layer. It was not possible to create the band fully in this layer due to limitations of the cell hardware. The shape and distribution of the Pt particles is very similar to the band formed in experiment 2. The band is symmetric with the most number of particles and majority of mass occurring in the same location. This means that the relationship between nucleation and particle growth are similar for these bands formed further from the cathode than experiment 1. It suggests that the proximity to the cathode has some sort of effect which has not been identified.

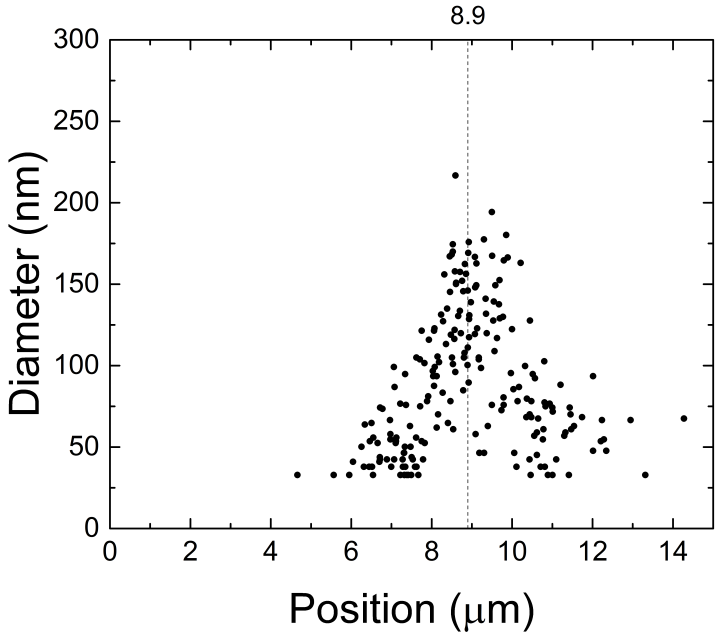


**Figure 36: Band formed in EPTFE layer with extra high oxygen crossover. Dotted line is predicted location using model**

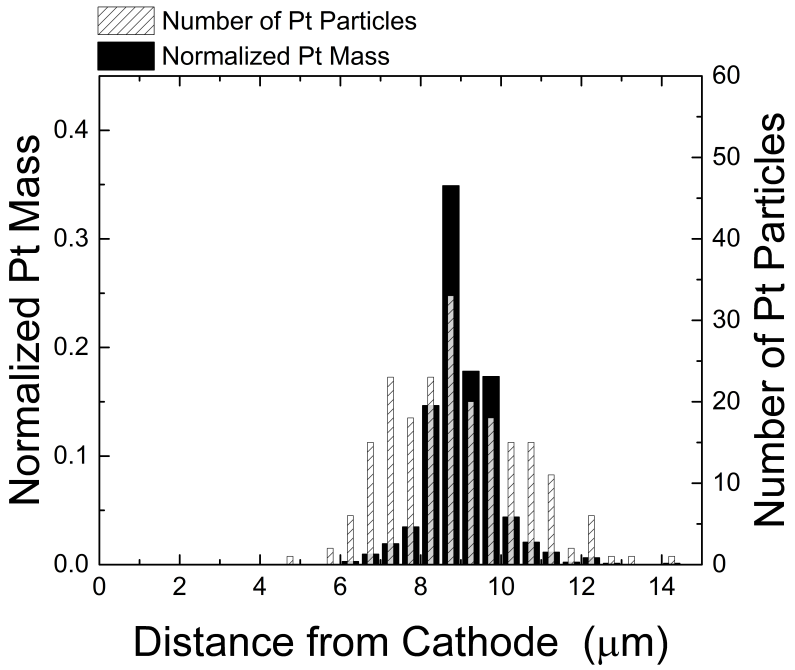


**Figure 37: Normalized mass and particle distribution for band formed in EPTFE layer**